

---

## Evidence of an ice-dammed lake outburst in the North Sea during the last deglaciation

Hjelstuen Berit Oline <sup>1,\*</sup>, Sejrup Hans Petter <sup>1</sup>, Valvik Espen <sup>1</sup>, Becker Lukas W. M. <sup>1</sup>

<sup>1</sup> Univ Bergen, Dept Earth Sci, Allegaten 41, N-5007 Bergen, Norway.

\* Corresponding author : Berit Oline Hjelstuen, email address : [berit.hjelstuen@uib.no](mailto:berit.hjelstuen@uib.no)

---

### Abstract :

Recent reconstructions suggest that the British-Irish and Fennoscandian ice sheets coalesced and covered the central and northern North Sea from ca. 26 cal. ka BP and until ca. 19 cal. ka BP. At ca. 19 cal. ka BP the Norwegian Channel Ice Stream started to retreat and the ice sheets broke apart at ca. 18.7 cal. ka BP. This led to a drainage of an ice-dammed lake in the southern North Sea northwards via the Norwegian Channel into the SE Nordic Seas. In this paper we combine information from high resolution TOPAS profiles, bathymetric records and shallow borings to study the ice-dammed lake outburst, a common deglaciation process but which rarely has been evidenced in such a detail from the marine realm. A 12 m deep and 3 km wide incision at the northeastern part of the Dogger Bank is suggested to represent the point where the ice-dammed lake breached. The glacial lake outburst flood, which had an estimated peak discharge of  $9.8 \times 10^4$ - $2.9 \times 10^5$  m<sup>3</sup>/s and lasted for about 5-15 months, flowed between the withdrawing British-Irish and Fennoscandian ice sheets following the crest of the Ling Bank northwards. Along this path, about 300 km downstream of the break-through point, an up to 10 m thick sediment package with a prograding-aggrading sedimentation pattern, typical for ice-dammed lake outburst deposits, has been deposited. This sediment package was deposited in a high-energy environment, immediately following extensive erosion of the underlying till unit of Last Glacial Maximum age. An oxygen isotope anomaly and an associated ultra-rapidly deposited meltwater plume on the Norwegian continental margin, dated to ca. 18.7 cal. ka BP, also witness this lake outburst. The ice-dammed lake outburst flood occurred when evidence suggest a sea level at least 110 m lower than at present in the region. As the sea level rose, following the melting of the Last Glacial Maximum ice sheet, the Ling Bank Delta developed on top the outburst deposits. The delta, indicating a sea level close to 80 m below present, has an extent of 80 km and up to 12 m deep fluvial channels are associated with the topset beds. This fluvial environment may have lasted until the end of the Younger Dryas time period when the Ling Bank was submerged and attained its present water depth.

---

## Highlights

► An ice-dammed lake existed in the southern North Sea during the Last Glacial Maximum. ► The ice-dammed lake outbursts at 18.7 cal. ka BP. ► The lake outburst had an estimated peak discharge of  $9.8 \times 10^4$ – $2.9 \times 10^5$  m<sup>3</sup>/s. ► The drainage lasted for about 5–15 months.

**Keywords** : North Sea, Ice-dammed lake, Glacial lake outburst flood, Last Glacial Maximum, Deglaciation, Delta

## 41 **1. Introduction**

42 Ice-dammed lakes develop supraglacially, subglacially or ice-marginally and their  
43 formation and length of existence are strongly dependent on the dynamics of the ice sheet and  
44 the character of the neighboring environment (Carrivick and Tweed, 2013). Well-studied  
45 examples of paleo ice-dammed lakes are Lake Agassiz (Laurentide Ice Sheet) which existed  
46 for a time period of 4000 years during the last deglaciation, the late Wisconsin Glacier Lake  
47 Missoula (Coredellian Ice Sheet), and the Younger Dryas Baltic Ice Lake (Scandinavian Ice  
48 Sheet) (e.g., Jensen et al., 1997; Teller et al., 2004; Alho et al., 2010). Such ice-dammed lakes  
49 can cover considerable areas and contain huge volumes of water. The 9700 km<sup>2</sup> Glacier Lake  
50 Missoula held a water volume of 2600 km<sup>3</sup>, whereas the Baltic Ice Lake was nearly four times  
51 larger in area and 10 times larger in volume (Teller et al., 2002; Jakobsson et al., 2007). On the  
52 other hand, Lake Agassiz covered a total area of 841,000 km<sup>2</sup> and contained a water volume  
53 of 163,000 km<sup>3</sup> when it merged with Lake Ojibway about 8200 years ago (Teller et al., 2002).

54 We note that the largest lake on Earth today, the Caspian Sea, covers 371,000 km<sup>2</sup> and has a  
55 volume of 78,200 km<sup>3</sup> (Rodionov, 2012).

56 Ice-dammed lakes can be drained, often periodically, and such glacial lake outburst floods  
57 (GLOFs) commonly represent abrupt discharges of large volumes of water. It has been  
58 estimated that the prominent 8.2 cal. ka BP drainage of Lake Agassiz was ongoing for 6  
59 months, with an average flux of 5 Sv, and involved a total water volume of 10<sup>14</sup> m<sup>3</sup> (Clarke et  
60 al., 2004). GLOFs are reported from onshore areas as canyons and giant gravel bars, whereas  
61 in the marine domain such sudden release of dense fresh water can give rise to prominent  
62 meltwater peaks in sediment cores (e.g., Alley and Ágústsdóttir, 2005; Høgaas and Longva,  
63 2016).

64 It is of importance to have knowledge on GLOFs, and their associated processes, as they  
65 give information on deglaciation character and as they may have a strong impact on climate  
66 and ocean circulation (Carriwick and Tweed, 2013). Notably, the around 1000 year-long  
67 Younger Dryas event has been suggested to be related to the 9500 km<sup>2</sup> Herman Drainage  
68 Stage of Lake Agassiz (Broecker et al., 1989; Teller et al., 2002). Smaller ice-dammed lakes  
69 are at present located on e.g. Iceland, in Scandinavia and in the Central European Alps and it  
70 is suggested that the number of such lakes will increase in the years to come due to the  
71 inferred warming climate (Carriwick and Tweed, 2016). Thus, outburst floods may increase in  
72 frequency and become an increasing threat to infrastructure and buildings.

73 In this study we will investigate the drainage route of a paleo-GLOF from an ice-dammed  
74 lake predicted by many authors (e.g., Hijma et al., 2012; Sejrup et al., 2016) to have existed  
75 during the Last Glacial Maximum (LGM) in the southern North Sea (Fig. 1), and which we  
76 here name the Late Weichselian North Sea Lake. In this effort we will integrate high  
77 resolution acoustic data and information from already analyzed shallow borings, and **(1)**  
78 identify outburst processes using seismic facies analyses, **(2)** evaluate seabed features and

79 their possible relationship with the GLOF, (3) study sediment character of identified seismic  
80 facies and seismic units, and (4) discuss a chronological framework for the identified  
81 processes. Finally, we will put the ice-dammed lake outburst in context of the late glacial-  
82 Holocene paleo-environmental history of the North Sea region.

83

## 84 **2. Background**

85 The epicontinental North Sea is characterized by water depths of <150 m except for in the  
86 Norwegian Channel, a prominent seabed depression along the south and west coast of  
87 Norway that reaches a maximum water depth of 700 m in the Skagerrak (Figs. 1-3). In  
88 general, the water depth in the North Sea shows a gradually increase from south to north.  
89 South of Dogger Bank the water depth does not exceed 60 m. North of Dogger Bank the  
90 North Sea is characterized by an embayment. This embayment reaches a maximum water  
91 depth of 150 m in the Fladen Basin and is bounded to the east by the Ling Bank (Figs. 2 and  
92 3). Several larger-sized rivers, including the Rhine, Elbe, Weser and Ems, are at present  
93 entering the southern North Sea (Fig. 1). The effect these rivers had on shaping the seabed  
94 morphology during glacial low sea level stands is easily visible in the bathymetric data (Fig.  
95 3a).

96 It has been suggested that the northern and central North Sea have been partly or fully ice  
97 covered several times during the Late Quaternary Northern Hemisphere Glaciations (Sejrup et  
98 al., 2005; Graham et al., 2011; Lee et al., 2012), and that the British-Irish (BIIS) and  
99 Fennoscandian (FIS) ice sheets coalesced in this region for the last time during the LGM  
100 (Clark et al., 2012; Sejrup et al., 2016). Evidence of these ice advances are imprinted in the  
101 sediment stratigraphy as moraine packages, and as networks of buried and exposed tunnel  
102 valleys (Sejrup et al., 1987; Sejrup et al., 1995; Stewart and Longergan, 2011). The last  
103 glacial-deglaciation cycle of the North Sea region is partly evidenced in the present day

104 seabed, which shows a complex pattern of ice marginal features, lateral shear zone moraines  
105 and glacial lineations (Fig. 3) (Bradwell et al., 2008; Sejrup et al., 2016).

106 During maximum glacial stages global eustatic sea level was around 120 m lower than  
107 today (e.g., Lambeck et al., 2014), and parts of the North Sea were located above sea level for  
108 some time after the withdrawal of the LGM ice sheet. Especially, the Dogger and Ling banks  
109 (Figs. 1 and 2) must have been sub-aerially exposed for a considerable time span, and these  
110 now “lost lands” have attracted strong interest as they in post-glacial time may have been sites  
111 for early settlements (e.g., Coles, 2000; Hammer et al., 2015).

112 It has been suggested that an ice-dammed lake has occupied the region south of Dogger  
113 Bank during various glacial stages, including Marine Isotope Stage (MIS) 12, MIS 6 and MIS  
114 2 (e.g., Hijma et al., 2012; Murton and Murton, 2012). The Late Weichselian North Sea Lake  
115 outburst was by Sejrup et al. (2016) suggested to follow an ice free corridor that existed  
116 between the BIIS and FIS as these ice sheets started to unzip, flowing into the Norwegian  
117 Channel through the proposed Ling Bank Drainage Channel (Fig. 1). Also a light spike in  
118 oxygen-isotopes in planktonic foraminifera, possibly reflecting large input of freshwater to  
119 the ocean, is identified close to 18.7 cal. ka BP in cores from the SE Nordic Seas margin  
120 (Lekens et al., 2005), and which probably reflect the Late Weichselian North Sea Lake  
121 drainage event (Sejrup et al., 2016). The ice-dammed lake has, based on maximum North Sea  
122 ice margins and bathymetric variations in the area, been estimated to be 3900 km<sup>3</sup> (Bigg et al.,  
123 2012). Thus, the Late Weichselian North Sea Lake is comparable to the proposed Late  
124 Wisconsin Glacier Lake Missoula in North America (Teller et al., 2002).

125

### 126 **3. Data and methods**

127 The data base used in this study includes TOPAS high resolution seismic profiles,  
128 bathymetric data and shallow borings (Figs. 2 and 3).

129 The seismic profiles, which have been collected during several University of Bergen  
130 cruises onboard R/V G.O. Sars between 2006 and 2014, define a broad grid within the study  
131 area (Fig. 2). During data acquisition, a TOPAS PS18 system from Kongsberg AS was used,  
132 giving seismic profiles with a vertical resolution of around 30 cm and a maximum penetration  
133 of ca. 100 m. The seismic profiles analyzed for this study have an overall good quality and  
134 were interpreted using the Petrel 2013 software from Schlumberger AS. We base the seismic  
135 interpretation on seismic facies character and changes in this throughout the study area.

136 An isopach map, in millisecond(two-way travel time) [ms(twt)], showing thickness and  
137 distribution of the sediments deposited in the Norwegian Channel between the last  
138 deglaciation (19-17.5 cal. ka BP) and the end of the Younger Dryas (11.6 cal. ka BP) has been  
139 generated. In addition to the TOPAS seismic profiles presented in this study, this map is also  
140 based on numerous other TOPAS lines collected in the Norwegian Channel (see Fig. 1a in  
141 Sejrup et al., 2016). For conversion of sediment thickness and sediment depth in ms(twt) to  
142 depth in meter, a velocity in the sediments of 1500 m/s has been applied.

143 The bathymetric database used in this study, Olex, has been made available by Olex AS  
144 ([www.olex.no](http://www.olex.no)). In Olex, individual data sets, acquired by fishing and research vessels, have  
145 been merged into a single database with a horizontal resolution of 5x5 m. The vertical  
146 resolution of the database is <1 m, and positioning errors are commonly less than 10 m. The  
147 Olex database has good coverage in the northern part of the North Sea, whereas regions with  
148 more scattered data coverage are identified in the central part and particularly in the southern  
149 part of the North Sea (Figs. 2 and 3). The analyses of the bathymetric data was done both in  
150 the Olex system, where the bathymetry can be viewed as 2D contours, 2D shaded relief, 3D  
151 views or as 2D profiles, and on exported .tiff files which were georeferenced and interpreted  
152 in the ArcGIS 10.3 software from Esri.

153 We have also utilized information from three previously analyzed shallow borings in the  
154 study area, B2001 (1.72°E-58.39°N), LH-BH3/4 (2.26°E-58.79°N) and 3/6-1 (4.89°E-  
155 56.58°N) (Fig. 2). B2001 was drilled in 110 m water depth and penetrated to a depth of 119.3  
156 m below the seabed, and information on the upper 20 m on grain-size, shear strength and  
157 chronology have previously been published by Sejrup et al. (1987) and Sejrup et al. (1994).  
158 Boring 3/6-1 was raised from a water depth of 64 m at the southern part of the Ling Bank  
159 (Fig. 2), and penetrates 37 m into the sediments. The upper 12 m of this boring has been sub-  
160 divided into five units based on grain size and various geotechnical parameters (Hammer et  
161 al., 2015). LN-BH3/4 is located in a water depth of 109 m at the northern tip of the Ling  
162 Bank, and information on grain size and shear strength are available from this borehole  
163 (Reinardy et al., 2017). In addition to these study area specific borings we have also used  
164 published information from sediment cores located elsewhere in the North Sea and on the  
165 Norwegian continental margin (Figs. 2 and 3).

166

## 167 **4. Results**

### 168 *4.1 Bathymetry and seabed character*

169 In the southernmost North Sea maximum water depths of 50 m is reached in an elongated  
170 bathymetric depression bounded by the coastlines of Denmark, Germany, the Netherlands and  
171 UK in east, west and south and the Dogger Bank to the north (Fig. 2). A ridge, standing up to  
172 10 m above the surrounding seabed, interrupts the otherwise rather flat sea floor of the  
173 depression (Fig. 2 and 3). Two prominent seabed incisions, Inc-I and Inc-II (Fig. 3), are  
174 observed at the western and eastern edges of the bathymetric depression. Inc-I has an east-  
175 west trend, is up to 30 km wide and reaches a maximum water depth of 83 m, whereas Inc-II  
176 has a maximum water depth of 56 m and a width of around 10-15 km.



177 The SW-NE trending Dogger Bank (Fig. 2) is a prominent elevated area located at the  
178 boundary between the southern and central North Sea. The bank has a length of nearly 300  
179 km in the E-W direction and is up to 100 km wide. The shallowest part of the Dogger Bank is  
180 located to the southwest, where the seafloor is situated only 11 m below the present day sea  
181 level. Towards the northeast the Dogger Bank is both narrowing and deepening, and at its  
182 northwestern tip, where the Dogger Bank is incised by Inc-II (Fig. 3), the water depth is  
183 around 40 m. The northern boundary of the Dogger Bank is characterized by an  $<0.2^\circ$  slope,  
184 along where the water depth is increasing from 40-50 m to approximately 60-80 m.

185 Northeast of the Dogger Bank is the Ling Bank located (Figs. 1 and 3). Along the crest of  
186 this bank the water depth is only 65 m, shallowing to 45 m across Store Fiskebank (Great  
187 Fisher Bank) (Figs. 2 and 3). Store Fiskebank resembles a typical moraine ridge shape, with a  
188 northern flank that is much steeper than the southern. The Ling Bank is approximate 200 km  
189 wide nearby Dogger Bank, narrowing to only around 40 km at its northern tip where a rather  
190 abrupt deepening in the water depth to 110-120 m, across a  $0.03^\circ$  slope, is observed (Fig. 3b).  
191 The slope of the Ling Bank towards the Norwegian Channel is as steep as  $0.6^\circ$ , whereas the  
192 western slope is gentler. East and west of the Ling Bank the water depth is around 80-90 m  
193 and the seabed is expressing a glacial landscape, where tunnel valleys, inclined ledges and ice  
194 marginal features have been identified (Sejrup et al., 2016). In the northern North Sea the  
195 seabed is dominated by a fresh glacial landscape (Bradwell et al., 2008; Sejrup et al., 2016),  
196 except for in the Fladen and Viking Bank basins areas (Fig. 3) where a relatively flat and  
197 smooth seabed in water depths of 150 m and 110 m is observed.

198

#### 199 *4.2 Seismic facies and sediment character*

200 Two seismic facies are dominating in the study area; acoustically transparent and  
201 acoustically well laminated. The acoustically transparent seismic facies has been shown to

202 represent till, as documented both by sediment core-seismic profile correlation in this study  
203 and by previous work in the region on similar data (e.g., Sejrup et al., 2015). The acoustically  
204 well laminated seismic pattern, comprising medium to high amplitude continuous and parallel  
205 reflectors are, based on a comparison to studies by Graham et al. (2010) and Sejrup et al.  
206 (2015), suggested to represent glacimarine deposits.

207

#### 208 *4.2.1 Area north of Ling Bank*

209 The region north of the Ling Bank comprises two prominent accumulation areas of  
210 postglacial sediments, the Fladen Basin and the not previously studied Viking Bank Basin  
211 (Fig. 2). The Fladen Basin contains an up to 25 m thick unit of acoustically well laminated  
212 glacimarine sediments which are interfingered by several glacial debris flows (Sejrup et  
213 al., 2015). The Viking Bank Basin covers an area of around 3500 km<sup>2</sup>, and contains an up to  
214 35 m thick sediment package that drapes one or several acoustically transparent till units (Fig.  
215 4). Several deep incisions, both exposed at the seabed and buried, are observed, and we infer  
216 these features to represent tunnel valleys. Tunnel valleys are commonly identified in the  
217 North Sea (e.g., Huuse and Lykke-Andersen et al., 2000). The acoustic data also show that the  
218 Viking Bank Basin is an area of shallow gas (Fig. 4), locally reducing the seismic penetration.  
219 The sediment package deposited in the Viking Bank Basin is characterized by an acoustically  
220 well laminated seismic facies, inferred to represent glacimarine sediments. However, in the  
221 uppermost 15-20 ms(twt) (ca. 12-15 m) of the deposited sequence a wavier and more  
222 contorted seismic pattern is identified. Furthermore, numerous point source reflectors are  
223 identified in this part of the sediment column, most likely representing more coarse-grained  
224 sediments.

225 At the northern tip of the Ling Bank, prominent changes in the seismic facies make us  
226 divide the sediment succession in this region into four sub-units, LBI (oldest) - LBIV (Figs. 5

227 and 6a). Sub-unit LBI comprises continuous, parallel medium to high amplitude reflectors and  
228 seems to represent classic glacimarine sediments deposited above a till unit. This till unit is,  
229 locally, defining the base of the Fladen and Ling Bank sediment basins, and can also easily be  
230 followed into the Norwegian Channel.

231 LBII reaches a maximum thickness of about 10 m, and is characterized by medium to  
232 high amplitude continuous reflections that define a prograding-aggrading seismic pattern (Fig.  
233 6a). This seismic facies cover an area of ca. 3400 km<sup>2</sup> (Fig. 3a), and can be followed for a  
234 distance of up to 40 km. At the base of sub-unit LBII several mounds, up to 5 m in height and  
235 2 km in diameter, are observed (Fig. 6b). Commonly, sub-unit LBII is overlying sub-unit LBI.  
236 We note, however, that LBII, locally, downlap the mapped till unit (Fig. 6a). In this  
237 downlapping region the surface of the till unit is extremely flat.

238 Sub-unit LBIII has been deposited stratigraphically above LBII, and is characterized by  
239 an acoustically contorted seismic facies where point-source reflectors are frequently identified  
240 (Fig. 5). Towards the Norwegian Channel this sediment package increases in thickness and  
241 incisions, up to 500 m in width and 5 ms(twt) (ca. 3.5 m) deep, are observed. These incisions  
242 are commonly observed at two levels in the sediment package. The uppermost identified sub-  
243 unit, LBIV, has an acoustically transparent to acoustically weakly layered character.

244 Shallow borings B2001 and LH-BH3/4 (Fig. 2) penetrate sub-units LBII-LBIV, and  
245 reveal that the observed changes in acoustic facies are mirroring lithology variations in the  
246 deposited sediment package (Fig. 7). Mapping of LBI-LBIV equivalent sediments in the  
247 Norwegian Channel shows that these deposits reach a maximum thickness of 160 ms(twt) (ca.  
248 120 m) in the Skagerrak region (Fig. 8). In the central part of the Norwegian Channel the  
249 sediment thickness is much less, reaching a maximum of 70 ms(twt) (ca. 50 m) in a  
250 depocentre along the western edge of the Norwegian Channel. The outermost part of the

251 Norwegian Channel is characterized by sediment thicknesses of less than 20 ms(twt) (ca. 15  
252 m).

253

#### 254 4.2.2. *Ling Bank*

255 Along the Ling Bank stacks of acoustically transparent units, which we suggest to  
256 represent till units, dominate the sub-seabed sediment succession (Fig. 9). Several major  
257 incisions, assumed to partly represent tunnel valleys, have eroded into these units. Still, these  
258 incisions have remnants of their presumed original sediment infill, represented by an  
259 acoustically well-laminated seismic facies, and which we infer to represent glacialmarine  
260 deposits (Fig. 9). However, mostly such possible infills have been removed and replaced by  
261 till packages.

262 At the northernmost part of the Ling Bank, in present water depths of 65-70 m, a unit  
263 composed of northward dipping clinoforms is identified (Figs. 3 and 10). The clinoforms are  
264 most likely representing topset, forset and possibly bottomset beds of a delta, which we name  
265 the Ling Bank Delta. The delta is about 80 km in length, up to 10 m thick and shows a well-  
266 defined pinch-out at its southern boundary. The TOPAS seismic profiles show indications of  
267 several incisions in the topset beds (Fig. 10). At the northern tip of the Ling Bank, the delta  
268 front seems to downlap the upper surface of sub-unit BFII, and the boundary between the  
269 downlapping clinoforms and sub-unit BFII are identified as a zone of high amplitude patches  
270 (Fig. 6a).

271 Along the crest of the Ling Bank, near the present day seabed, three incisions are  
272 identified (Figs. 3, 9a and 9b). These incisions have eroded 10-20 ms(twt) (7-15 m) into the  
273 sub-seabed sediment succession and can be traced for up to 6 km in the available seismic  
274 profiles. A draping or prograding infill style characterizes these features.

275 At the southern part of the Ling Bank, at the boundary towards the Dogger Bank, the  
276 present day current system in the region have caused sand waves and sand dunes to develop,  
277 prohibiting seismic penetration with the TOPAS system (Fig. 11a). The TOPAS seismic  
278 profiles, however, reveal a 20 ms(twt) (ca. 15 m) deep cut in the sediment succession at the  
279 location where a prominent bathymetric depression is observed (Inc-II in Fig. 3c). In this  
280 region we also observe erosion of the surrounding sediment packages (Fig. 11a). Southeast of  
281 Store Fiskebank, in an area where glacial imprints in the seabed are not observed, we identify  
282 erosion of the surface of the uppermost identified till unit (Figs. 3 and 11b). Furthermore, the  
283 sub-bottom data show that a less than 10 ms(twt) (ca. 7 m) thick sediment package, displaying  
284 the same prograding pattern as sub-unit LBII further north, has been deposited in this region.  
285 Boring 3/6-1 (Hammer et al., 2015) indicates that this sediment package is dominated by  
286 sand.

287

## 288 **5. Discussion**

### 289 *5.1 Acoustic evidence of a lake outburst flood, its transport route and its dimensions*

290 The studied bathymetric and seismic data give several indications about both the existence  
291 of a GLOF in the North Sea and the transport route it followed after the collapse of the lake-  
292 supporting ice-barrier. A strong evidence is the identified seismic sub-unit LBII, mapped at  
293 the northern tip of the Ling Bank (Figs. 3, 5 and 6a). The observed northward prograding  
294 direction of this unit (Fig. 6a) suggests that LBII has had a southerly source, which is in line  
295 with the existence of an ice-dammed lake south of Dogger Bank (Fig. 1). The prograding-  
296 aggrading character of this unit also typically resembles the depositional nature of lake-  
297 outburst deposits, as are reported from field studies of terrestrial GLOFs (Russell et al., 2001;  
298 Smith, 2006; Carling et al., 2013).

299 Seismic sub-unit LBII is in the study area, furthermore, overlying a seismically  
300 homogenous unit which, based on seismic characteristics and information from cores in the  
301 region (Fig. 7), has been identified as till or glacially overridden sediments representing the  
302 last glacial phase in the area. The boundary of the till towards LBII is characterized by a very  
303 flat and smooth surface when comparing it with regions where LBI is deposited on top of this  
304 unit (Fig. 5). This relationship between LBII deposits and the flat surface make us infer that  
305 sub-unit LBII during deposition had a strong erosion capacity, and reshaped the upper  
306 boundary of the till to a smooth and slightly westward dipping surface in an approximately  
307 2200 km<sup>2</sup> large area (Figs. 3a and 5). This inferred high-sedimentation rate environment is  
308 also supported by the seismic signature observed near the bottom of LBII. Here, smaller-sized  
309 mounds are observed, and which, when comparing to land-based field data from GLOFs in  
310 NW Germany (Fig. 16 in Meinsen et al., 2011), may represent convoluted bedding formed  
311 during high energy deposition. We note that erosional boundaries between GLOF deposits  
312 and underlying strata are frequently reported from land-based studies (e.g., Hanson and  
313 Calgue, 2016). Alho et al. (2010) have also, from a paleohydraulic drainage reconstruction of  
314 Glacier Lake Missoula, shown that the shear stress affecting the bed during a GLOF is high  
315 and capable of eroding the substrata. Thus, the combined observation of erosion, its location,  
316 at the till-LBII boundary, and the character of BFII suggests that this unit is related to a lake  
317 outburst flood. Similar indications of outburst sediments and erosion are observed at the  
318 southern part of the Ling Bank (Figs. 3 and 11b).

319 We note that there is a distance of about 300 km from the assumed Late Weichselian North  
320 Sea Lake (Fig. 1) and the sediments in LBII, but large travel distances seem to be common for  
321 GLOFs. During the Glacier Lake Missoula drainage, outburst flood features covered distances  
322 of up to 700 km (Hansson et al., 2012). Two borings, B2001 and LN-BH3/4, penetrate the  
323 assumed GLOF deposits at the tip of the Ling Bank (Figs. 2, 5 - 7), documenting that 40-60%

324 of the outburst sediments consist of sand and coarser material, indicating high energy  
325 environments. The borings further indicate that the GLOF deposits represent an upward-  
326 coarsening sequence. However, the relative low core recovery, and also the distance between  
327 borings and seismic profiles (up to 5 km) should call for some caution. Boring 3/6-1 (Figs. 2  
328 and 3) (Hammer et al., 2015), suggest a similar composition of the possible outburst  
329 sediments on the southern Ling Bank, noting that this assumption is based on only one  
330 sediment sample from these deposits.

331 Our bathymetric data give further evidence for the pathway of the outburst. At the NE part  
332 of the Dogger Bank the water depth is reaching a maximum of 56 m, and the seafloor is thus  
333 lying about 15 m deeper than the surrounding areas (Inc-II in Fig. 3c). We infer that this  
334 seabed depression represents the transport pathway that developed when the ice-barrier broke,  
335 causing the GLOF to flow northwards. The seabed morphology (Fig. 3a) also suggests that  
336 this region of the North Sea has been a lake-outburst point, showing the same characteristic  
337 features as found in a DTM (Digital Terrain Model) from the Lower Rhine Embayment where  
338 a moraine ridge has been dissected by a Middle Pleistocene glacial lake outburst flood (Lang  
339 and Winsemann, 2013). It should, however, be noted that the TOPAS seismic profiles reveal  
340 that large regions in the southern North Sea is draped by post-glacial deposition of cover sand  
341 and sand waves, thereby concealing some of the drainage features in bathymetric maps.  
342 Across the observed bathymetric incision (Inc-II in Fig. 3) our sub-bottom data also reveal an  
343 infilled 15 m deep and 3000 m wide depression with associated erosional surfaces at its flanks  
344 (Fig. 11a). This adds supporting evidence that this region at the NE part of the Dogger Bank  
345 represents the out-burst point of the ice dammed lake.

346 Thus, based on observations in the available acoustic data we infer that the Late  
347 Weichselian North Sea Lake had a catastrophic drainage and formed a prominent seabed/sub  
348 seabed incision at the NE part of the Dogger Bank (Figs. 3c and 11b). The outburst flood

349 followed the Ling Bank east of Store Fiskebank (Fig. 3a) northwards before depositing unit  
350 LBII (Fig. 6a) at the northernmost tip of the Ling Bank. By utilizing equation  $Q = V \times 0.5(A_1$   
351  $+ A_2) \times H$ , where  $Q$  is peak discharge ( $m^3/s$ ),  $V$  is velocity ( $m/s$ ),  $A_1$  and  $A_2$  is minimum and  
352 maximum width ( $m$ ) of the outburst channel and  $H$  is the pass height ( $m$ ), a first estimate of  
353 the flood discharge can be calculated in a similar way as has been demonstrated by Meinsen  
354 et al. (2011) for a Saalian glacial outburst flood in NW Germany.

355 A pass height of 6 m and channel widths of 555 m (channel bottom), 1500 m and 3000 m  
356 (channel top) were utilized to calculate discharge for two depth intervals (0-6 m and 6-12 m)  
357 of the assumed break-out channel (Fig. 11a). We used 5 and 15 m/s, which is suggested to be  
358 characteristic velocities for GLOFs (Baker, 2009), as a minimum and maximum velocity.  
359 Thus, a peak discharge in the range of  $9.8 \times 10^4 m^3/s$  -  $2.9 \times 10^5 m^3/s$  is estimated for the Late  
360 Weichselian North Sea Lake, suggesting that this outburst is a “major” jökulhlaup (see  
361 Meinsen et al. (2011) and references herein for classification system of jökulhlaup). The  
362 estimated discharge of the Late Weichselian North Sea Lake is similar to that of Glacier Lake  
363 Nedre Glomsjø in southeast Norway (Høgaas and Longva, 2016), but ten times less than the  
364 calculated discharge of the Glacier Lake Missoula (Alho et al., 2010).

365 If utilizing the estimated lake volume of  $3900 km^3$  (Bigg et al., 2012) it took between 5 and  
366 15 months to drain the Late Weichselian North Sea Lake.

367

## 368 *5.2 Late Glacial – Holocene paleo-environmental history*

369 It has been suggested that between ca. 26 and ca. 19 cal. ka BP the central and northern  
370 North Sea was covered by the BIIS and FIS, with a southern ice margin at the Dogger Bank  
371 and the northern at the present day shelf edge (Figs. 1, 12 and 13) (Sejrup et al., 2016, Becker  
372 et al., this issue). During this time period the Late Weichselian North Sea Lake is possibly  
373 draining southwards, through the English Channel (Toucanne et al., 2010).



374 In the Norwegian Channel the Norwegian Channel Ice Stream (NCIS) was operating,  
375 transporting huge amounts of sediments to the North Sea Fan (Figs. 1 and 13) (Sejrup et al.,  
376 2003; Nygård et al., 2005; Nygård et al., 2007; Hjelstuen et al., 2012). These sediments were  
377 transported downslope as glacigenic debris flows (GDFs), considered to represent signature  
378 deposits for shelf edge located ice streams (King et al., 1996). At ca. 19 cal. ka BP the last  
379 pulse of GDF activity is recorded at the North Sea Fan (King et al., 1998; Nygård et al.,  
380 2007), and the NCIS started to retreat into the Norwegian Channel. Soon after NCIS had left  
381 its position at the shelf edge, an up to 20 m thick fine-grained unit had been deposited along  
382 the Norwegian margin (e.g., Hjelstuen et al., 2004) (Figs. 1, 12 and 13). Age constrains from  
383 several IMAGES cores along the Norwegian margin (Fig. 1) reveal that this unit was  
384 deposited nearly instantaneously, at ca. 18.7 cal. ka BP (Lekens et al., 2005; Becker et al., this  
385 issue). It was earlier assumed that this unit, interpreted to be a meltwater plume, was related to  
386 the withdrawal and rapid melting of the NCIS (Sejrup et al., 2003; Hjelstuen et al., 2004;  
387 Lekens et al., 2005). We now suggest, however, that this meltwater flux is closely related to  
388 the sudden drainage of the Late Weichselian North Sea Lake. Seismic correlation of the till  
389 unit identified at the northern tip of the Ling Bank (Figs. 5 and 6) to shallow borings in the  
390 Fladen Basin (Fig. 2) suggests that it is related to the LGM. The observed deep erosion of this  
391 unit and the undisturbed outburst sediments superimposed (Figs. 5 and 6a) also evidence that  
392 the GLOF must have occurred in relation to the last deglaciation of the central and northern  
393 North Sea.

394 Thus, we follow the reconstruction of Sejrup et al. (2016) suggesting that there was a  
395 corridor between the BIIS and FIS at ca. 18.7 cal. ka BP, allowing for transportation of GLOF  
396 sediments and freshwater to the SE Nordic Seas (Fig. 13). As the GLOF entered the  
397 Norwegian Channel, through the proposed Ling Bank Drainage Channel, it flowed along the  
398 western edge of the retreating NCIS. The ice stream was at this time located about 200 km

399 inside the Norwegian Channel, close to the location of boring 8903 (Figs. 3 and 13). The  
400 observation of a grounding zone wedge in this region (Sejrup et al., 2016; Morén et al., in  
401 review) indicates that the NCIS stood still at this location for a period before it continued to  
402 retreat.

403 If taking sea level into account, using the eustatic sea level curve of Lambeck et al.  
404 (2014), it seems that the Late Weichselian North Sea Lake related GLOF sediments were  
405 deposited above sea level (Fig. 12). However, it should be noted that the North Sea have been  
406 influenced by a combined effect of glacioisostatic uplift and subsidence during the latest part  
407 of the Quaternary (Sejrup et al., 1987; Sejrup et al., 1998), making it challenging to envisage  
408 the exact sea level in the North Sea at a given time. Eustatic sea level curves should thus only  
409 be considered as a first approximation when evaluating paleo-environments in the North Sea.

410 After a time period of up to 15 months, which is based on estimated peak discharge and  
411 lake volume in the present study, the Late Weichselian North Sea Lake was drained. Notably,  
412 Lekens et al. (2005) counted 854 laminae, deposited in a rhythmic pattern, in the assumed  
413 meltwater plume deposits on the southern Vøring Plateau (Figs. 1 and 13). If assuming the  
414 rhythmic lamina pattern to represent tidal influence on an ice-dammed lake outburst, the  
415 drainage of the Late Weichselian North Sea Lake is close to have taken 15 months (854  
416 laminae represents 900 tidal cycles, or about 450 days). Thus, this supports the findings in this  
417 work. Following this assumed short-lived outburst event the NCIS continued its retreat  
418 through the Norwegian Channel, and by 17.6 cal. ka BP the NCIS had withdrawn to a position  
419 in the innermost Skagerrak (Morén et al., in review). Larger parts of the central and northern  
420 North Sea are now suggested to be ice free, with an ice cap over the British and the Shetland  
421 islands extending into the Fladen Basin region (Clark et al., 2012; Becker et al., this issue).

422 After the glacial ice-dammed lake outburst event a fluvial depositional environment  
423 developed in the study area, as evidenced by the build-up of the Ling Bank Delta at the

424 northern part of the Ling Bank (Figs. 3, 10, 12 and 13). We interpret the observed incisions at  
425 a shallow depth beneath the present day seabed (Fig. 9) to be channels in a meandering river  
426 system, transporting sediments to the steadily growing delta. The characteristic sediment infill  
427 pattern of these incisions (Fig. 9b) also supports their association with a river system (e.g.,  
428 Toonen et al., 2012). The assumed GLOF break-through point, at the NE part of the Dogger  
429 Bank (Fig. 11a), was also presumably used by rivers after the drainage of the Late  
430 Weichselian North Sea Lake.

431 Borings B2001 and LN-BH3/4 (Figs. 3 and 7) also evidence the changes in depositional  
432 environments after the Late Weichselian North Sea Lake outburst event. Sediments with a  
433 sand content of up to 80% are now deposited, suggested to reflect the input of fluvial-  
434 dominated sediments. Based on inspection of seismic facies character, where we infer that  
435 coarse grained sediments are reflected in the seismic data as point source reflectors, it seems  
436 that such sediments were deposited in a wide area north of the Ling Bank including the  
437 Viking Bank Basin (Figs. 3 and 4). The thick sediment depocentre at the western edge of the  
438 Norwegian Channel (Fig. 8) also seems mostly to be build up by fluvial deposits feed through  
439 the Ling Bank delta system. This assumption is based on analyze results from boring 8903  
440 (Fig. 2) (Sejrup et al., 1994) and interpretation of the acoustic data, which indicate that  
441 sediments related to the GLOF and the withdrawal of the NCIS only are represented as a thin,  
442 uniform sediment package in this region.

443 After the break-up and withdrawal of the BIIS and FIS from the main study area, the FIS  
444 margin was located along the coast of Norway until the start of the Allerød time period, at ca.  
445 14 cal. ka BP. Then the ice sheet continued to withdraw onshore with a short-lived terrestrial  
446 readvance during the Younger Dryas (e.g., Mangerud et al., 2011). Throughout this time  
447 period the sea level was rising, but with observed still stands at around 15 cal. ka BP, 13.5 cal.  
448 ka BP (Allerød) and 12 cal. ka BP (Younger Dryas) (Fig. 12). We note that the ca. 1000 year-

449 long halt in the sea level rise at around 15 cal. ka BP seems to coincide with the level of  
450 identified high-amplitude patches at the Ling Bank Delta front (Figs. 6a and 12), suggesting  
451 that these features may be related to a shoreline and an associated beach zone.

452 The fluvial-dominated environment within the central North Sea, including a period with  
453 an active delta system on the Ling Bank, may have lasted for almost 7000 years until the Ling  
454 Bank submerged at the end of the Younger Dryas time period (Fig. 12).

455

## 456 **6. Conclusions**

457 Based on high resolution acoustic records and information from shallow borings we have  
458 mapped the pathway and processes related to a glacial lake outburst flood in the North Sea.

459 The main findings are:

460

- 461 • The existence of a Late Weichselian North Sea Lake outburst is evidenced from:
  - 462 - An incision, about 12 m deep and 3000 m wide, at the NE part of the Dogger Bank.  
463 This incision is located in a water depth of about 56 m and is thought to represent the  
464 break-through point of the ice-dammed lake.
  - 465 - A prograding-aggrading unit (BFII) deposited at the northern tip of the Ling Bank  
466 which resembles typical characteristics of GLOF deposits. A similar depositional  
467 pattern is also observed on the southernmost part of the Ling Bank.
  - 468 - Erosional surfaces in glacial sediments are associated with the identified prograding-  
469 aggrading sediment sequences. Such surfaces are commonly associated with GLOFs.
- 470 • Dates from the North Sea and the continental slope suggest that the outburst took place at  
471 ca. 18.7 cal. ka BP. The flood followed the Ling Bank northwards for about 300 km  
472 before depositing an up to 10 m thick prograding-aggrading unit (BFII) at the northern tip  
473 of the Ling Bank. A meltwater plume and an associated meltwater spike, observed in

474 sediment cores and acoustic data from the Norwegian continental margin, are suggested to  
475 represent the far-field evidence of the GLOF.

- 476 • A first approximation in estimating GLOF peak discharge resulted in values between  $9.8 \times$   
477  $10^4$  and  $2.9 \times 10^4$  m<sup>3</sup>/s, indicating that the Late Weichselian North Sea Lake outburst is a  
478 “major” jökulhlaup. Thus, the discharge of the Late Weichselian North Sea Lake appears  
479 to be about 10 times smaller than that estimated for Glacier Lake Missoula.
- 480 • The Late Weichselian North Sea Lake is estimated to have drained in 5-15 months.
- 481 • The Late Weichselian North Sea Lake GLOF event was followed by a fluvial-dominated  
482 environment, where the Ling Bank Delta built up at the northern part of the Ling Bank  
483 during a rising sea level. A meandering river system seems to have existed in association  
484 with this delta. This fluvial environment may have existed as long as 7000 years, until the  
485 end of the Younger Dryas time period when the Ling Bank got submerged.

486

#### 487 **Acknowledgements**

488 We thank Jørgen Bergeland for mapping of post-LGM sediments in the Norwegian  
489 Channel and for generating the isopach map in Figure 8. The captains and crews onboard R/V  
490 G.O.Sars are thanked for all help during several UiB cruises to the North Sea, collecting data  
491 for this study. We also thank Olex AS, Trondheim, who gave us permission to use their  
492 bathymetric database. This study has been supported by the European Union’s Seventh  
493 Framework Programme FP7/2007–2013/ under the REA (Research Executive Agency) grant  
494 agreement 317217, the GLANAM ITN (Glaciated North Atlantic Margins Initial Training  
495 Network).

496

497

498

499 **References**

- 500 Alho, P., Baker, V.R., Smith, L.N., 2010. Paleohydraulic reconstruction of the largest Glacial  
501 Lake Missoula draining(s). *Quat. Sci. Rev.* 29(23), 3067-3078.
- 502 Alley, R.B., Ágústsdóttir, A.M., 2005. The 8k event: cause and consequences of a major  
503 Holocene abrupt climate change. *Quat. Sci. Rev.* 24(10), 1123-1149.
- 504 Baker, V.R., 2009. High-energy megafloods: planetary settings and sedimentary dynamics, in:  
505 Martini, P.I., Baker, V.R., Garzon, G. (Eds.), *Flood and megaflood processes and*  
506 *deposits: recent and ancient examples. Special Publication of the International*  
507 *Association of Sedimentologists*, 32. Blackwell Science, Oxford, pp. 3-15.
- 508 Becker, L.W.M., Sejrup, H.P., Hjelstuen, B.O., Haflidason, H., Dokken, T.M. Ocean - ice  
509 sheet interaction along the SE Nordic Seas margin from 35 - 15 ka BP. *Marine Geology*.  
510 This issue.
- 511 Bigg, G.R., Clark, C.D., Greenwood, S.L., Haflidason, H., Hughes, A.L.C., Levine, R.C.,  
512 Nygård, A., Sejrup, H.P., 2012. Sensitivity of the North Atlantic circulation to break-up  
513 of marine sectors of the NW European ice sheets during the last Glacial: A synthesis of  
514 modelling and palaeoceanography. *Global Planet. Change* 98-99, 153-165.
- 515 Bradwell, T., Stoker, M.S., Golledge, N.R., Wilson, C.K., Merritt, J.W., Long, D., Everest,  
516 J.D., Hestvik, O.B., Stevenson, A.G., Hubbard, A.L., Finlayson, A.G., Mathers, H.E.,  
517 2008. The northern sector of the last British Ice Sheet: Maximum extent and demise.  
518 *Earth-Sci. Rev.* 88, 207-226.
- 519 Broecker, W.S., Kennett, J.P., Flower, B.P., Teller, J.T., Trumbore, S., Bonani, G., Wolfli,  
520 W., 1989. Routing of meltwater from the Laurentide Ice Sheet during the Younger  
521 Dryas cold episode. *Nature* 341, 318-321.
- 522 Carling, P.A., 2013. Freshwater megaflood sedimentation: What can we learn about generic  
523 processes? *Earth-Sci. Rev.* 125, 87-113.

524 Carrivick, J.L., Tweed, F.S., 2013. Proglacial lakes: character, behaviour and geological  
525 importance. *Quat. Sci. Rev.* 78, 34-52.

526 Carrivick, J.L., Tweed, F.S., 2016. A global assessment of the societal impacts of glacier  
527 outburst floods. *Global Planet. Change* 144, 1-16.

528 Clark, C.C., Hughes, A.L.C., Greenwood, S.L., Jordan, C., Sejrup, H.P., 2012. Pattern and  
529 timing of the last British-Irish Ice Sheet. *Quat. Sci. Rev.* 44, 112-146.

530 Clarke, G.K., Leverington, D.W., Teller, J.T. and Dyke, A.S., 2004. Paleohydraulics of the  
531 last outburst flood from glacial Lake Agassiz and the 8200BP cold event. *Quat. Sci.*  
532 *Rev.* 23(3), 389-407.

533 Coles, B.J., 2000. Doggerland: the cultural dynamics of a shifting coastline. *Geol. Soc.*  
534 *London Spec. Pub.* 175(1), 393-401.

535 Graham, A.G., Stoker, M.S., Lonergan, L., Bradwell, T., Stewart, M.A., 2011. The  
536 Pleistocene glaciations of the North Sea Basin, in: Ehlers, J., Gibbard, P.L., Hughes,  
537 P.D., (Eds.), *Quaternary glaciations: extent and chronology: a closer look*. Elsevier, pp.  
538 261-278.

539 Graham, A.G., Lonergan, L., Stoker, M.S., 2010. Depositional environments and chronology  
540 of Late Weichselian glaciation and deglaciation in the central North Sea. *Boreas* 39(3),  
541 471-491.

542 Haflidason, H., Sejrup, H.P., Nygård, A., Mienert, J., Bryn, P., Lien, R., Forsberg, C.F., Berg,  
543 K., Masson, D., 2004. The Storegga Slide: architecture, geometry and slide  
544 development. *Mar. Geol.* 213, 201-234.

545 Hammer, Ø., Planke, S., Hafeez, A., Hjelstuen, B.O., Faleide, J.I., Kvalø, F., 2015. Agderia –  
546 a postglacial lost land in the southern Norwegian North Sea. *Nor. J. Geol.* 96, 43-60.

547 Hanson, M.A., Clague, J.J., 2016. Record of glacial Lake Missoula floods in glacial Lake  
548 Columbia, Washington. *Quat. Sci. Rev.* 133, 62-76.

549 Hanson, M.A., Lian, O.B., Clague, J.J., 2012. The sequence and timing of large late  
550 Pleistocene floods from glacial Lake Missoula. *Quat. Sci. Rev.* 31, 67-81.

551 Hijma, M.P., Cohen, K.M., Roebroeks, W., Westerhoff, W.E., Busschers, F.S., 2012.  
552 Pleistocene Rhine–Thames landscapes: geological background for hominin occupation  
553 of the southern North Sea region. *J. Quat. Sci.* 27(1), 17-39.

554 Hjelstuen, B.O., Nygård, A., Sejrup, H.P., Haflidason, H., 2012. Quaternary denudation of  
555 southern Fennoscandia - evidence from the marine realm. *Boreas* 41(3), 379-390.

556 Hjelstuen, B.O., Sejrup, H.P., Haflidason, H., Nygård, A., Berstad, I.M., Knorr, G., 2004.  
557 Late Quaternary seismic stratigraphy and geological development of the south Vøring  
558 margin, Norwegian Sea. *Quat. Sci. Rev.* 23, 1847-1865.

559 Høgaas, F., Longva, O., 2016. Mega deposits and erosive features related to the glacial lake  
560 Nedre Glomsjø outburst flood, southeastern Norway. *Quat. Sci. Rev.* 151, 273-291.

561 Huuse, M., Lykke-Andersen, H., 2000. Overdeepened Quaternary valleys in the eastern  
562 Danish North Sea: morphology and origin. *Quat. Sci. Rev.* 19(12), 1233-1253.

563 Jakobsson, M., Björck, S., Alm, G., Andrén, T., Lindeberg, G., Svensson, N.O., 2007.  
564 Reconstructing the Younger Dryas ice dammed lake in the Baltic Basin: Bathymetry,  
565 area and volume. *Global Planet. Change* 57(3), 355-370.

566 Jensen, J.B., Bennike, O., Witkowski, A., Lemke, W., Kuijpers, A., 1997. The Baltic Ice Lake  
567 in the southwestern Baltic: sequence, chrono- and biostratigraphy. *Boreas* 26(3), 217-  
568 236.

569 King, E.L., Haflidason, H., Sejrup, H.P., Løvlie, R., 1998. Glacigenic debris flows on the  
570 North Sea Trough Mouth Fan during ice stream maxima. *Mar. Geol.* 152, 217-246.

571 King, E.L., Sejrup, H.P., Haflidason, H., Elverhøi, A., Aarseth, I. 1996. Quaternary seismic  
572 stratigraphy of the North Sea Fan: Glacially-fed gravity flow aprons, hemipelagic  
573 sediments, and large submarine slides. *Mar. Geol.* 130, 293-315.



574 Lambeck, K., Rouby, H., Purcell, A., Sun, Y., Sambridge, M., 2014. Sea level and global ice  
575 volumes from the Last Glacial Maximum to the Holocene. *Proc. National Academy of*  
576 *Science* 111(43), 15296-15303.

577 Lang, J., Winsemann, J., 2013. Lateral and vertical facies relationships of bedforms deposited  
578 by aggrading supercritical flows: from cyclic steps to humpback dunes. *Sed. Geol.* 296,  
579 36-54.

580 Lee, J.R., Busschers, F.S., Sejrup, H.P., 2012. Pre-Weichselian Quaternary glaciations of the  
581 British Isles, The Netherlands, Norway and adjacent marine areas south of 68°N:  
582 implications for long-term ice sheet development in Northern Europe. *Quat. Sci. Rev.*  
583 44, 213-228.

584 Lekens, W.A.H., Sejrup, H.P., Haflidason, H., Petersen, G.Ø., Hjelstuen, B.O., Knorr, G.,  
585 2005. Laminated sediments preceding Heinrich event 1 in the Northern North Sea and  
586 Southern Norwegian Sea; origin, processes and regional linkage. *Mar. Geol.* 216, 27-50.

587 Mangerud, J., Gyllencreutz, R., Lohne, Ø., Svendsen, J. I., 2011. Glacial history of Norway,  
588 in: Ehlers, J., Gibbard, P.L., Hughes, P.D., (Eds.), *Quaternary glaciations: extent and*  
589 *chronology: a closer look*. Elsevier, pp 279-298.

590 Meinsen, J., Winsemann, J., Weitkamp, A., Landmeyer, N., Lenz, A., Dölling, M., 2011.  
591 Middle Pleistocene (Saalian) lake outburst floods in the Münsterland Embayment (NW  
592 Germany): impacts and magnitudes. *Quat. Sci. Rev.* 30(19), 2597-2625.

593 Morén, B.M., Sejrup, H.P., Hjelstuen, B.O., Borge, M.V., Schäuble, C. The last deglaciation  
594 of the Norwegian Channel; geomorphology, stratigraphy and radiocarbon dating.  
595 *Boreas*. In review

596 Murton, D.K., Murton, J.B., 2012. Middle and Late Pleistocene glacial lakes of lowland  
597 Britain and the southern North Sea Basin. *Quat. Int.* 260, 115-142.

598 Nygård, A., Sejrup, H. P., Haflidason, H., Bryn, P., 2005. The glacial North Sea Fan, southern  
599 Norwegian Margin: Architecture and evolution from the continental slope to the deep-  
600 sea basin. *Mar. Pet. Geol.* 22, 71-84.

601 Nygård, A., Sejrup, H.P., Haflidason, H., Lekens, W.A.H., Clark, C.D., Bigg, G.R., 2007.  
602 Extreme sediment and ice discharge from marine-based ice streams: New evidence from  
603 the North Sea. *Geology* 35, 395-398.

604 Reinardy, B.T., Hjelstuen, B.O., Sejrup, H.P., Augedal, H., Jørstad, A., 2017. Late Pliocene-  
605 Pleistocene environments and glacial history of the northern North Sea. *Quat. Sci. Rev.*,  
606 158, 107-126.

607 Rodionov, S.N., 2012. Global and regional climate interaction: the Caspian Sea experience.  
608 Springer Science and Business Media, ISBN 978-94-010-4468-4, 242 pp.

609 Russell, A.J., Knudsen, O., Fay, H., Marren, P.M., Heinz, J., Tronicke, J., 2001. Morphology  
610 and sedimentology of a giant supraglacial, ice-walled, jökulhlaup channel,  
611 Skeiðarárjökull, Iceland: implications for esker genesis. *Global Planet. Change* 28(1),  
612 193-216.

613 Sejrup, H.P., Clark, C.D., Hjelstuen, B.O., 2016. Rapid ice sheet retreat triggered by ice  
614 stream buttressing: Evidence from the North Sea. *Geology* 44(5), 355-358.

615 Sejrup, H.P., Haflidason, H., Aarseth, I., King, E., Forsberg, C.F., Long, D., Rokoengen, K.,  
616 1994. Late Weichselian glaciation history of the northern North Sea. *Boreas* 23, 1-13.

617 Sejrup, H.P., Hjelstuen, B.O., Dahlgren, K.I.T., Haflidason, H., Kuijpers, A., Nygård, A.,  
618 Praeg, D., Stoker, M.S., Vorren, T.O., 2005. Pleistocene glacial history of the NW  
619 European continental margin. *Mar. Pet. Geol.* 22, 1111-1129.

620 Sejrup, H.P., Hjelstuen, B.O., Nygård, A., Haflidason, H., Mardal, I., 2015. Late Devensian  
621 ice marginal features in the central North Sea – processes and chronology. *Boreas* 44, 1-  
622 13.

623 Sejrup, H.P., Landvik, J.Y., Larsen, E., Janocko, J., Eiriksson, J., King, E., 1998. The Jæren  
624 Area; a Border Zone of the Norwegian Channel Ice Stream. *Quat. Sci. Rev.* 17, 801-  
625 812.

626 Sejrup, H.P., Larsen, E., Haflidason, H., Berstad, I.M., Hjelstuen, B.O., Jonsdottir, H.E.,  
627 King, E.L., Landvik, J., Longva, O., Nygård, A., Ottesen, D., Raunholm, S., Rise, L.,  
628 Stalsberg, K., 2003. Configuration, history and impact of the Norwegian Channel Ice  
629 Stream. *Boreas* 32, 18-36.

630 Sejrup, H.P., Aarseth, I., Ellingsen, K.L., Reither, E., Jansen, E., Løvlie, R., Bent, A.,  
631 Brigham-Grette, J., Larsen, E., Stoker, M.S., 1987. Quaternary stratigraphy of the  
632 Fladen area, central North Sea: A multidisciplinary study. *J. Quat. Sci.* 2, 35-58.

633 Sejrup, H.P., Aarseth, I., Haflidason, H., Løvlie, R., Bratten, Å., Tjøstheim, G., Forsberg, C.F.,  
634 Ellingsen, K.I., 1995. Quaternary of the Norwegian Channel: glaciation history and  
635 palaeoceanography. *Nor. J. Geol.* 75, 65-87.

636 Smith, L.N., 2006. Stratigraphic evidence for multiple drainings of glacial Lake Missoula  
637 along the Clark Fork River, Montana, USA. *Quat. Res.* 66, 311-322.

638 Stewart, M.A., Lonergan, L., 2011. Seven glacial cycles in the middle-late Pleistocene of  
639 northwest Europe: Geomorphic evidence from buried tunnel valleys. *Geology* 39(3),  
640 283-286.

641 Teller, J.T., Leverington, D.W., Mann, J.D., 2002. Freshwater outbursts to the oceans from  
642 glacial Lake Agassiz and their role in climate change during the last deglaciation. *Quat.*  
643 *Sci. Rev.* 21(8), 879-887.

644 Teller, J.T., Leverington, D.W., 2004. Glacial Lake Agassiz: A 5000 yr history of change and  
645 its relationship to the  $\delta^{18}\text{O}$  record of Greenland. *Geol. Soc. Am. Bull.* 116(5-6), 729-  
646 742.

647 Toonen, W.H., Kleinhans, M.G., Cohen, K.M., 2012. Sedimentary architecture of abandoned  
648 channel fills. *Earth Surf. Proc. Landforms* 37(4), 459-472.

649 Toucanne, S., Zaragosi, S., Bourillet, J.F., Marieu, V., Cremer, M., Kageyama, M., Van Vliet-  
650 Lanoë, B., Eynaud, F., Jean-Louis Turon, J.-L., Gibbard, P.L., 2010. The first  
651 estimation of Fleuve Manche palaeoriver discharge during the last deglaciation:  
652 evidence for Fennoscandian ice sheet meltwater flow in the English Channel ca 20–18  
653 ka ago. *Earth Planet. Sci. Let.* 290(3), 459-473.

654

655

656

657

658

659

660

661

662

663

664

665

666

667

668

669

670

671

672

673 **Figure caption**

674

675 **Figure 1. a)** Overview map of North Sea and Norwegian continental margin. Outlines of  
676 meltwater plume deposits on the south Vøring Plateau (from Hjelstuen et al., 2004), Late  
677 Weichselian North Sea Lake, Dogger Bank, Ling Bank, Ling Bank Drainage Channel (from  
678 Sejrup et al. [2016]), North Sea Fan (from Nygård et al. [2005]), Storegga Slide (from  
679 Haflidason et al. [2004]) and LGM ice extend (based on Sejrup et al. [2005]) are shown.  
680 Location of major rivers entering the southern North Sea and sediment cores mentioned in  
681 this study are also indicated. SS: Storegga Slide; NSF: North Sea Fan; LBDC: Ling Bank  
682 Drainage Channel; DB: Dogger Bank; LB: Ling Bank; LGM: Last Glacial Maximum.

683

684 **Figure 2.** North Sea bathymetric map based on the Olex bathymetric database  
685 ([www.olex.no](http://www.olex.no)). Location of shallow borings, sediment cores and TOPAS seismic profiles  
686 applied or mentioned in this study are shown (For full TOPAS seismic database see Fig. 1a in  
687 Sejrup et al. [2016]). DB: Dogger Bank; SF: Store Fiskebank (Great Fisher Bank); LB: Ling  
688 Bank; FB: Fladen Basin; VBB: Viking Bank Basin; VB: Viking Bank; NC: Norwegian  
689 Channel; RE: River Elbe; RW: River Weser; RE: River Ems.

690

691 **Figure 3. a)** 3D bathymetric view, based on the Olex bathymetric database, of southern and  
692 central North Sea. Location of Ling Bank Delta, channels and ice-dammed lake outburst  
693 sediments are indicated. DB: Dogger Bank; SF: Store Fiskebank (Great Fisher Bank); LB:  
694 Ling Bank; FB: Fladen Basin; VBB: Viking Bank Basin; VB: Viking Bank; NC: Norwegian  
695 Channel; TV: Tunnel valley; Inc: Incision; IL: Inclined ledge (from Sejrup et al. [2016]); IFP:  
696 Ice front position (based on Sejrup et al. [2016]); RE: River Elbe; RW: River Weser; RE: River Ems.

697 River Ems. **b)** and **c)** Bathymetric profiles across the Dogger and Ling banks. For location see  
698 Fig. 3a. The profiles are generated from the Olex bathymetric database.

699

700 **Figure 4.** TOPAS profile across Viking Bank Basin. Profile location in Fig. 3a. G: Gas; GM:  
701 Glacimarine sediments; F: Fluvial-dominated sediments; TV: Tunnel valley.

702

703 **Figure 5.** TOPAS seismic profile across the northern tip of Ling Bank showing typical  
704 seismic facies characters in this area. Profile location in Fig. 3a. LBI-LBIV and T: Identified  
705 seismic units.

706

707 **Figure 6. (a)** TOPAS seismic profile, location in Fig. 3a, showing assumed lake outburst  
708 deposits (LBII) north of Ling Bank. Note also the delta front pinch out. LBI-LBIV and T:  
709 Identified seismic units. **(b)** Zoom-in on ice dammed lake-outburst deposits. Arrows point at  
710 observed mounds at the base of sub-unit LBII. Figure location in Fig. 6a.

711

712 **Figure 7.** Lithology, grain size and shear strength of LGM moraine and post-LGM sediments  
713 (from Sejrup et al. (1994) [B2001] and Reinardy et al. (2017) [LN-BH3/4]). (\*) Age  
714 information from Sejrup et al. (2016). Correlation to seismic units identified in this study (T  
715 and LBII-IV) is indicated. Please note the long correlation distance of 5 km between B2001  
716 and the seismic profile (Fig. 5), which results in the upper and lower boundaries of seismic  
717 units only being inferred. Si: Silt; C: Clay; S: Sand; G: Gravel; GM: Glacimarine; F: Fluvial;  
718 M: Marine.

719

720 **Figure 8.** Isopach map in ms(twt) of sediments deposited in the Norwegian Channel between  
721 ca. 19 cal. ka BP (end LGM) and ca. 11.6 cal. ka BP (start of the Holocene). Black dot shows

722 location of boring 8903. LB: Ling Bank, VBB: Viking Bank Basin, VB: Viking Bank, FB:  
723 Fladen Basin, LBDC: Ling Bank Drainage Channel.

724

725 **Figure 9. (a)** TOPAS seismic example showing typical seismic stratigraphy, including tunnel  
726 valleys, possible river channels, glacial marine sediments (GM) and till units, across the Ling  
727 Bank. Profile location in Fig. 3a. **(b)** TOPAS seismic example highlighting sediment infill in  
728 an assumed river channel observed at the crest of the Ling Bank. Profile location in Fig. 3a.

729

730 **Figure 10.** TOPAS seismic profile from the northern part of the Ling Bank, showing the  
731 presumed Ling Bank Delta with bottomset, foreset and topset beds. Profile location in Fig. 3a.

732

733 **Figure 11. (a)** Sub-seabed incision observed at the Inc-II bathymetric low at the northeastern  
734 part of Dogger Bank. Location of TOPAS seismic profile in Fig. 3a. **(b)** Seismic facies  
735 character northwest of Store Fiskebank. Location of TOPAS seismic profile in Fig. 3a.

736

737 **Figure 12.** Post-glacial sea level curve, from Lambeck et al. (2014). Main glacial events,  
738 post-glacial processes, and depth to significant surfaces observed in the seismic profiles are  
739 indicated. Numbers (i) - (ii) - (iii) refer to time slices shown in Figure 13. Note change in  
740 horizontal scale. NC: Norwegian Channel; NCIS: Norwegian Channel Ice Stream; BIIS:  
741 British-Irish Ice Sheet; FIS: Fennoscandian Ice Sheet; LGM; Last Glacial Maximum.

742

743 **Figure 13.** Conceptual models for selected time slices of the Late glacial-Holocene paleo-  
744 environmental development of the North Sea. **(i) LGM.** Confluence of the British-Irish (BIIS)  
745 and Fennoscandian (FIS) ice sheets in the North Sea and formation of the Late Weichselian  
746 North Sea ice-dammed lake (LWNSL) south of Dogger Bank (DB). Location of boring 8903

747 (red dot) and drainage direction of LWNSL are indicated (open black arrow). LB: Ling Bank;  
748 NCIS: Norwegian Channel Ice Stream; GDF: Glacigenic Debris Flow. **(ii) 18.7 cal. ka BP.**  
749 Initiation of Late Weichselian North Sea Lake (LWNSL) outburst, deposition of outburst  
750 sediments (LBII) at the northern tip of Ling Bank and meltwater flux along the Norwegian  
751 margin. Ling Bank Drainage Channel indicated with a red arrow. GZW: Grounding Zone  
752 Wedge; NCIS: Norwegian Channel Ice Stream; FIS: Fennoscandian Ice Sheet; BIIS: British-  
753 Irish Ice Sheet. **(iii) 13 cal. ka BP.** Build-up of Ling Bank Delta, meandering rivers across  
754 Ling Bank and development of fluvial depocentre in the Norwegian Channel. Indicated  
755 shoreline is drawn approximately along present day 80 m water depth contour.  
756  
757



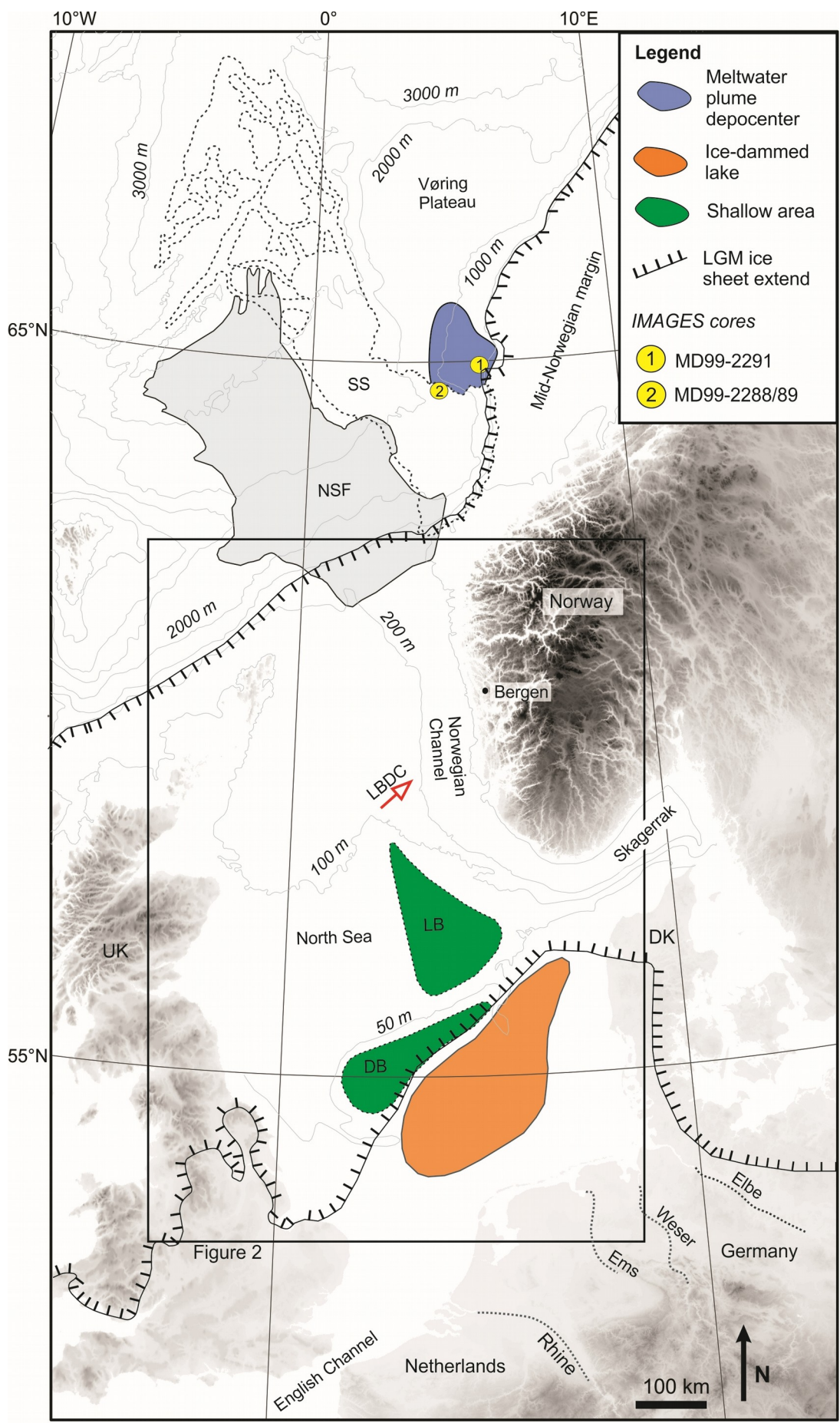


Figure 1. Hjelstuen et al.

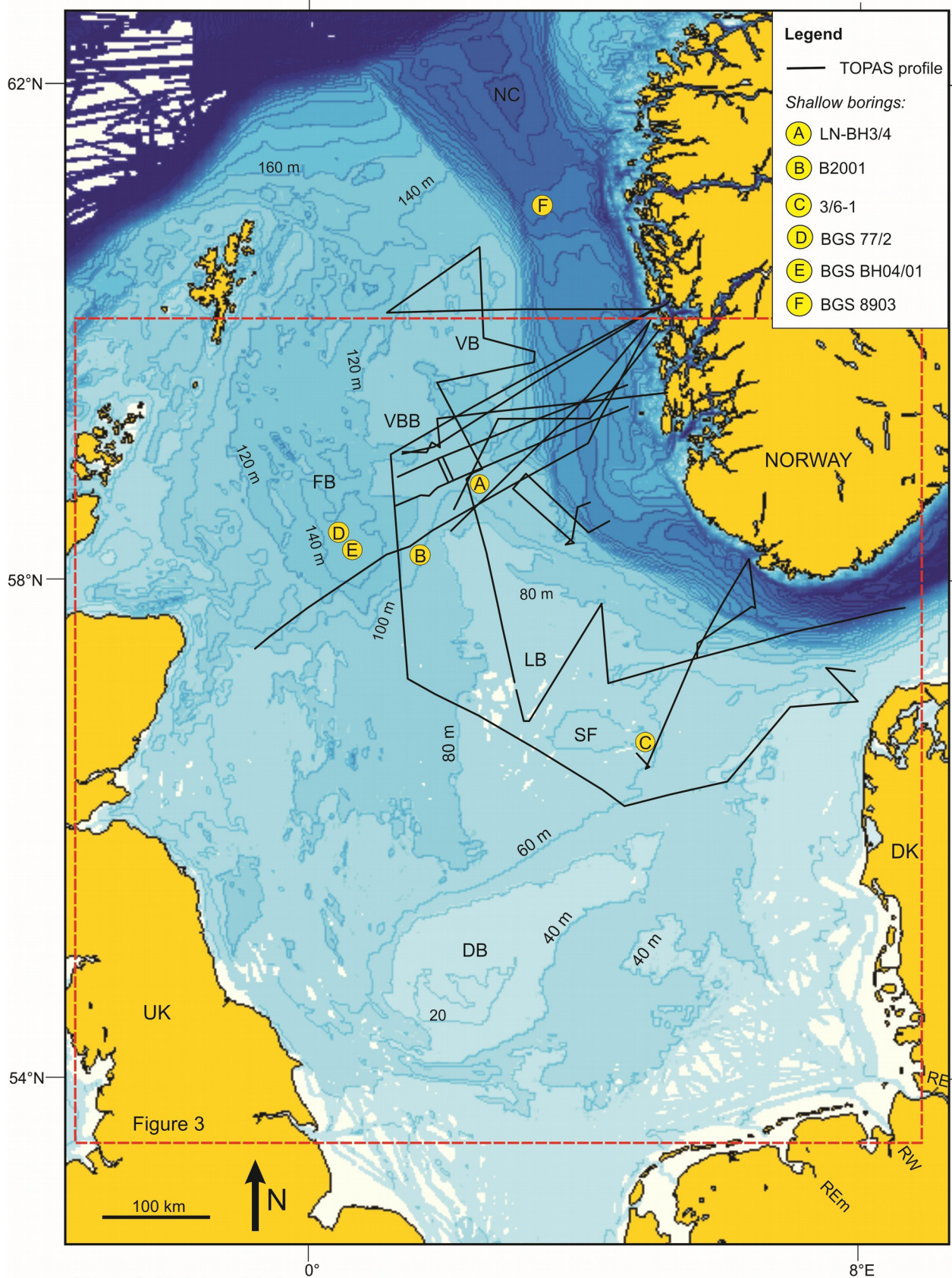


Figure 2. Hjelstuen et al.



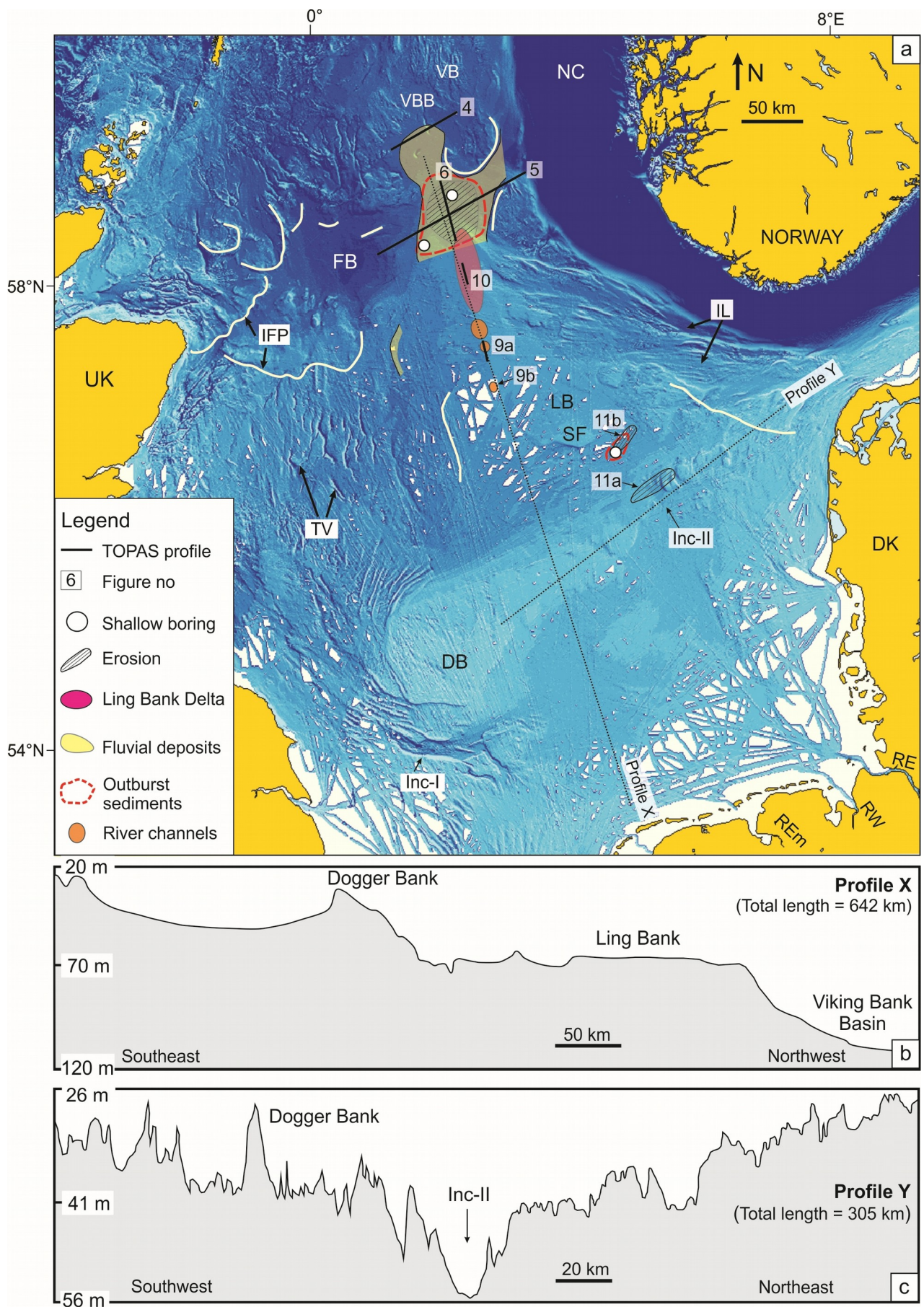


Figure 3. Hjelstuen et al.



Figure 4. Hjelstuen et al.



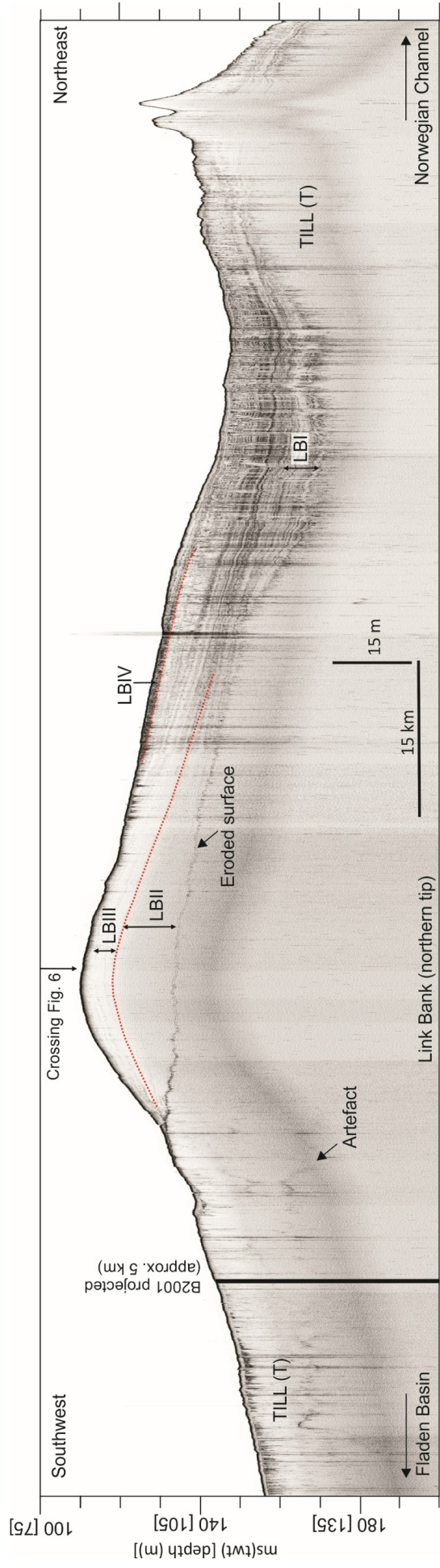


Figure 5. Hjelstuen et al.

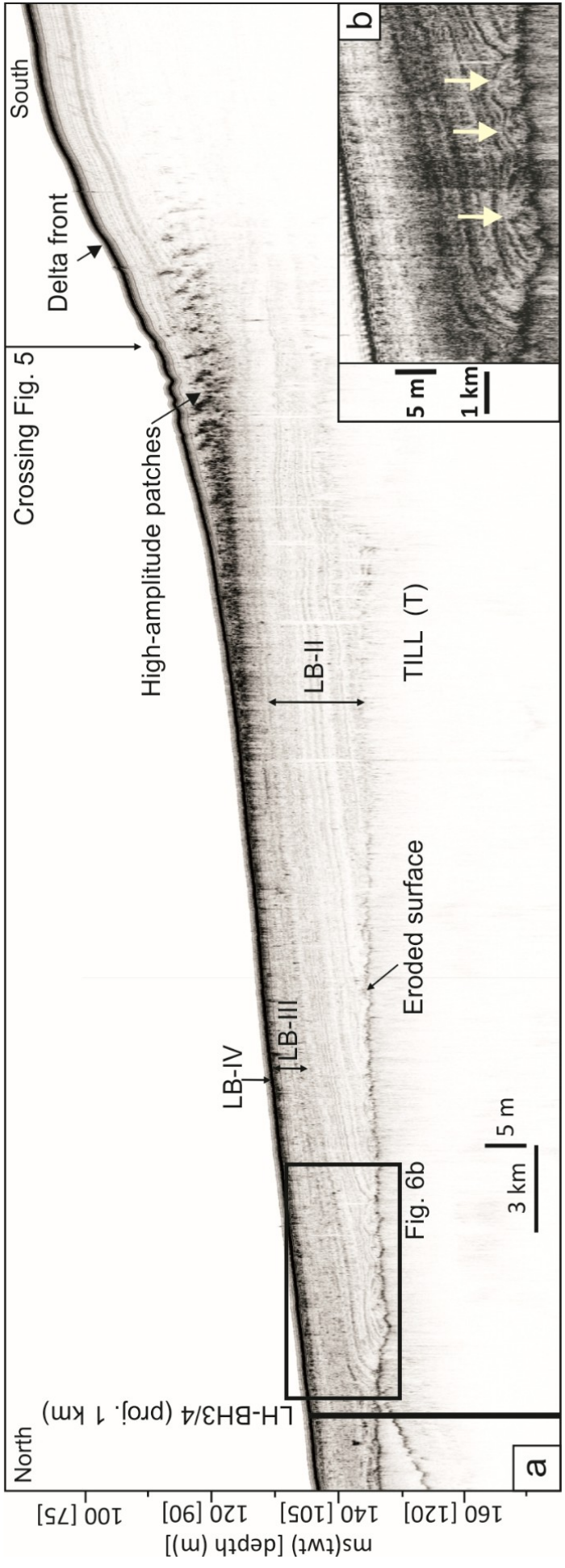
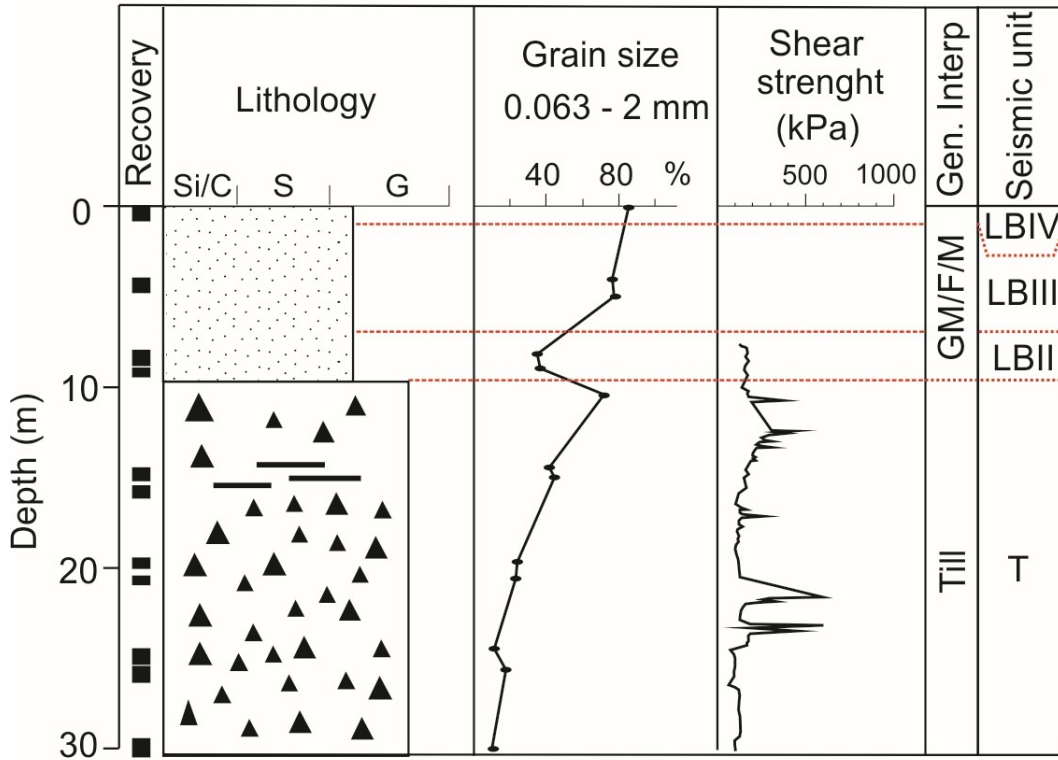


Figure 6. Hjelstuen et al.

LN-BH3/4 (1 km east of correlating seismic profile)



B2001 (5 km south off correlating seismic profile)

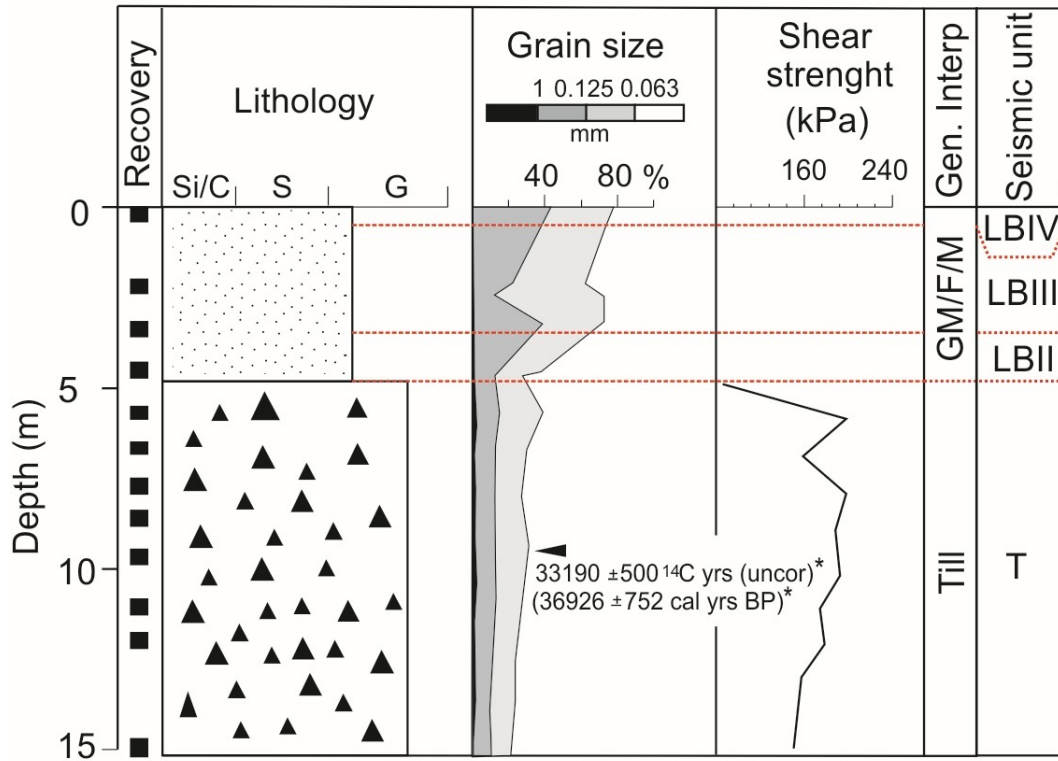


Figure 7. Hjelstuen et al.



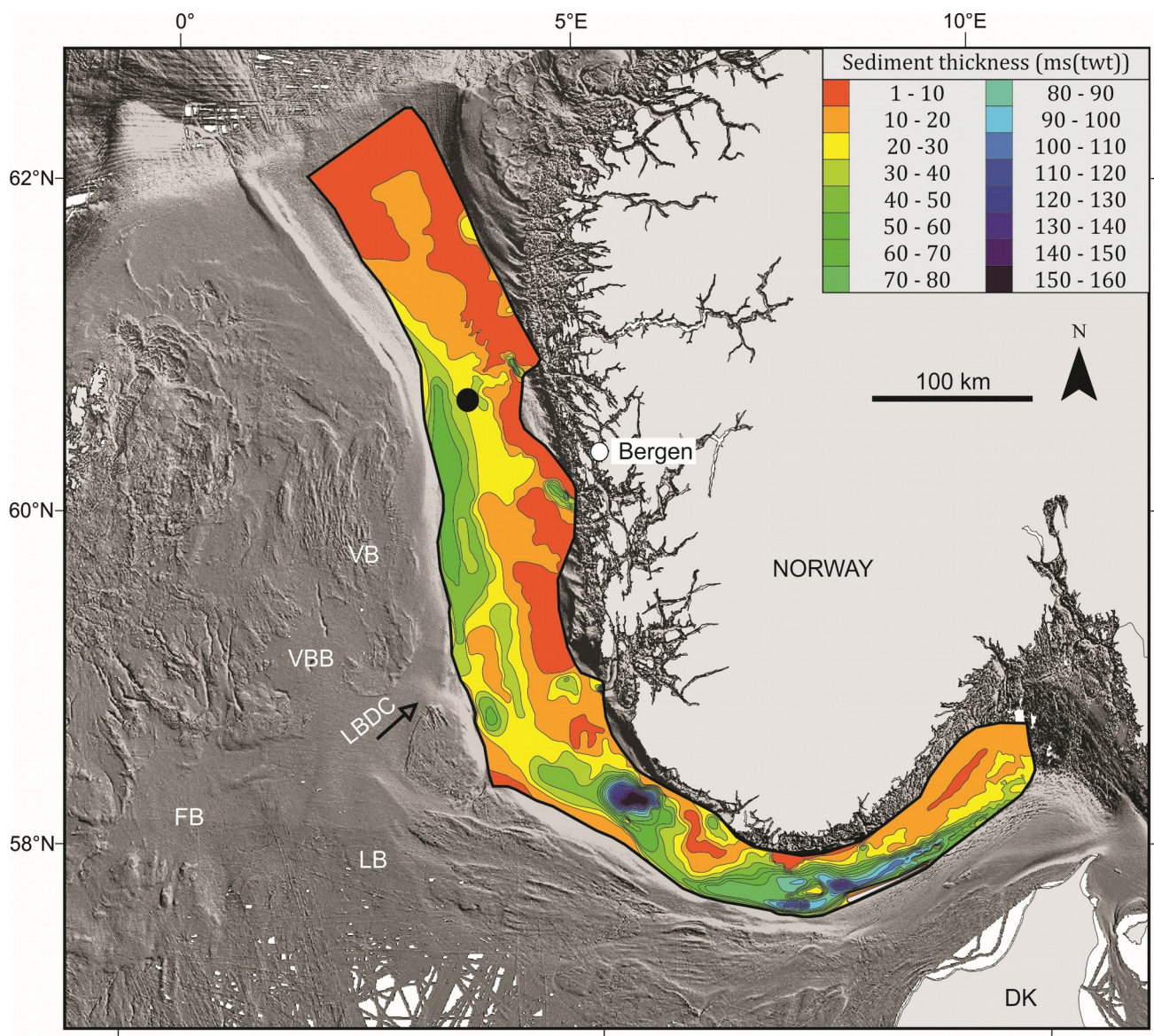


Figure 8. Hjelstuen et al



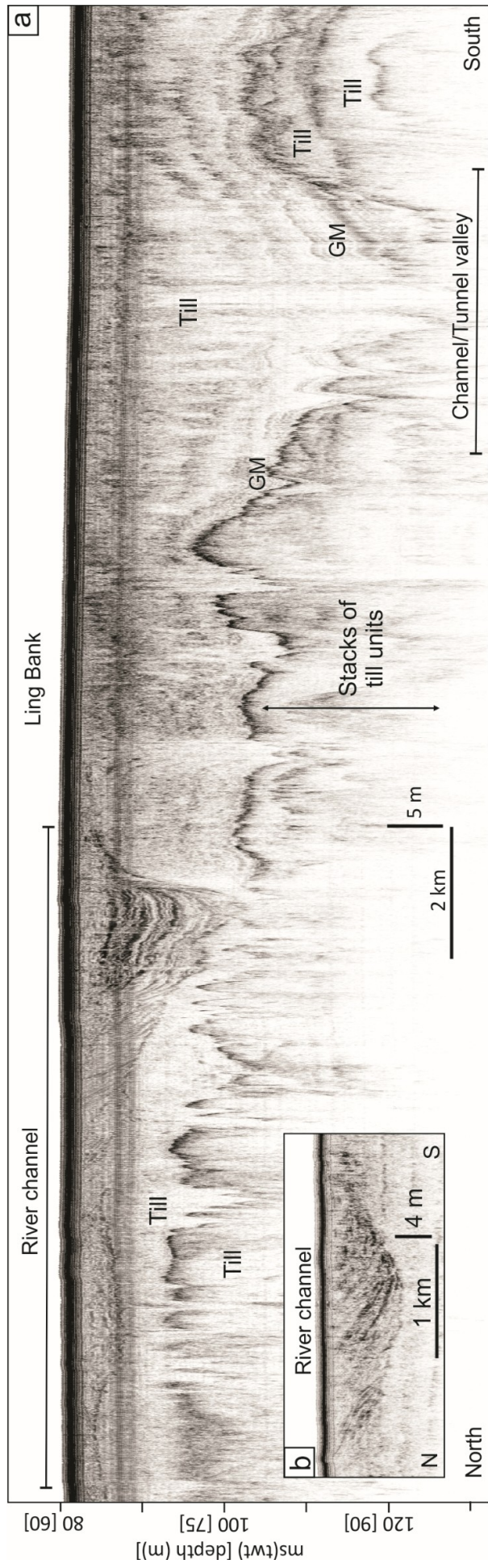


Figure 9. Hjelstuen et al.

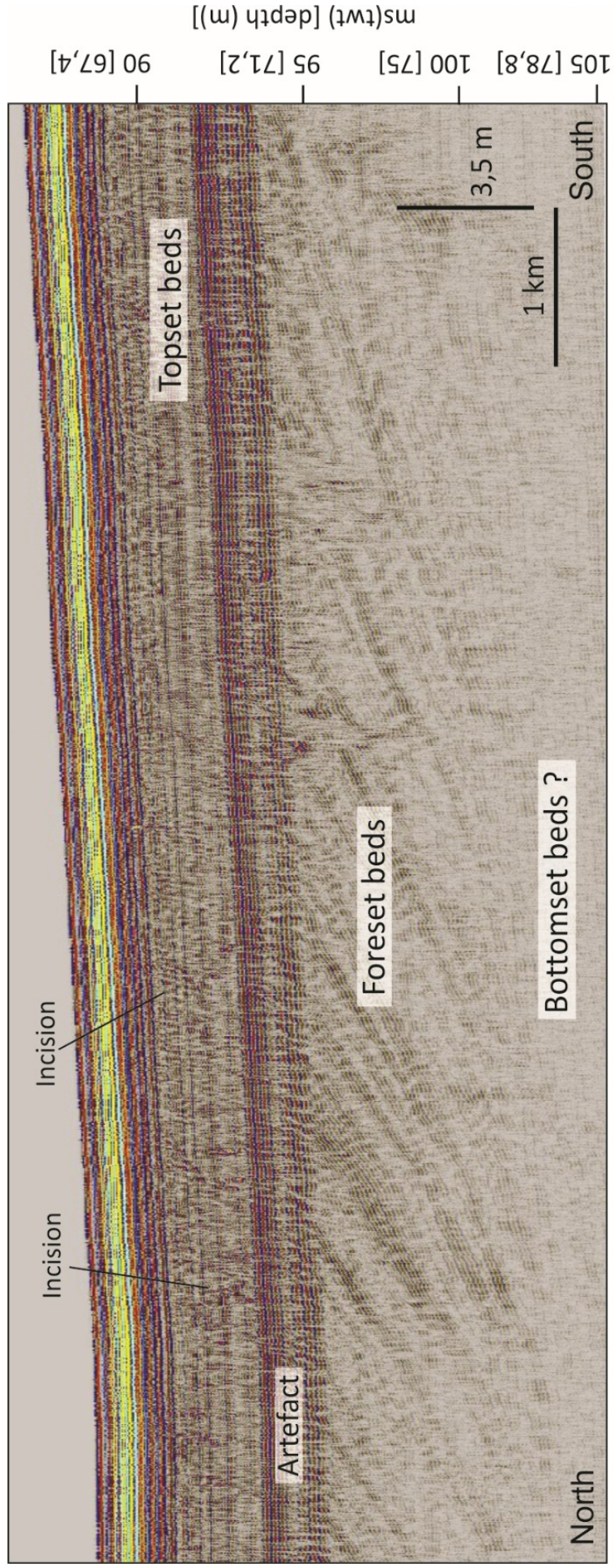


Figure 10. Hjelstuen et al.



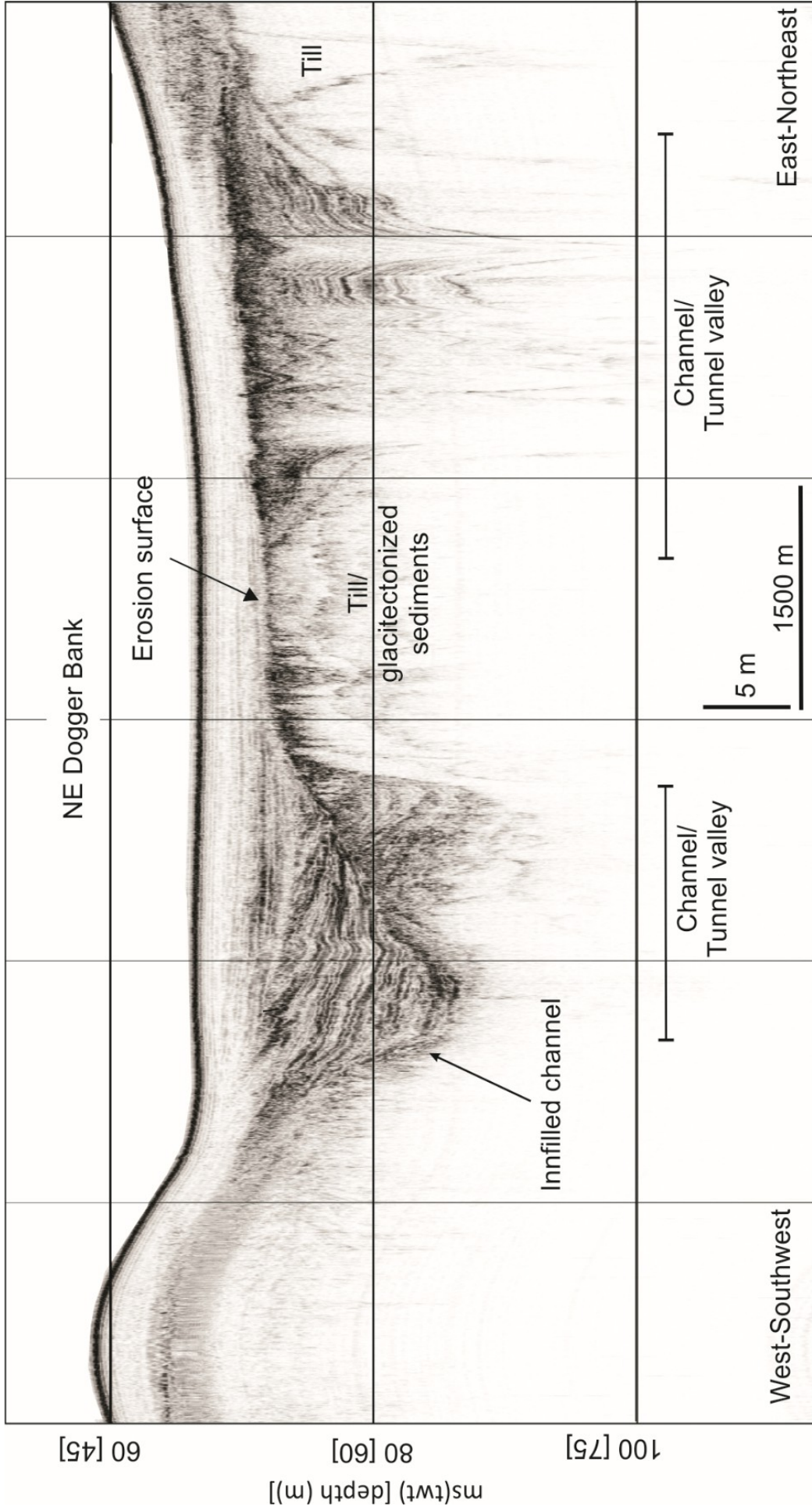


Figure 11a. Hjelstuen et al.

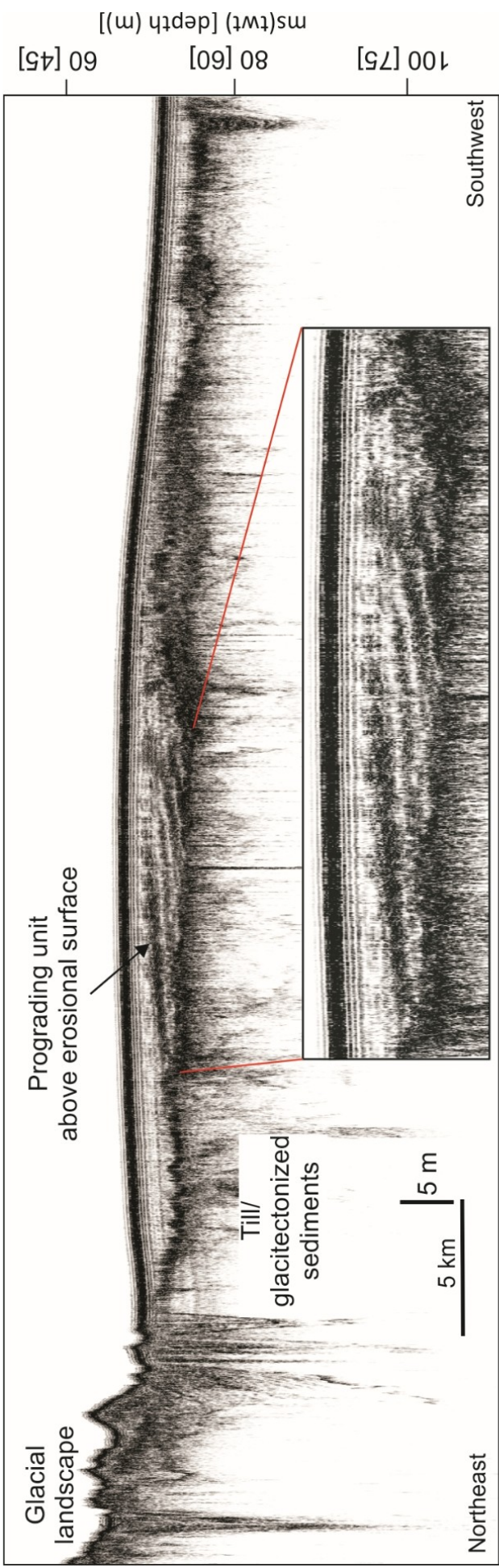


Figure 11b. Hjelstuen et al.

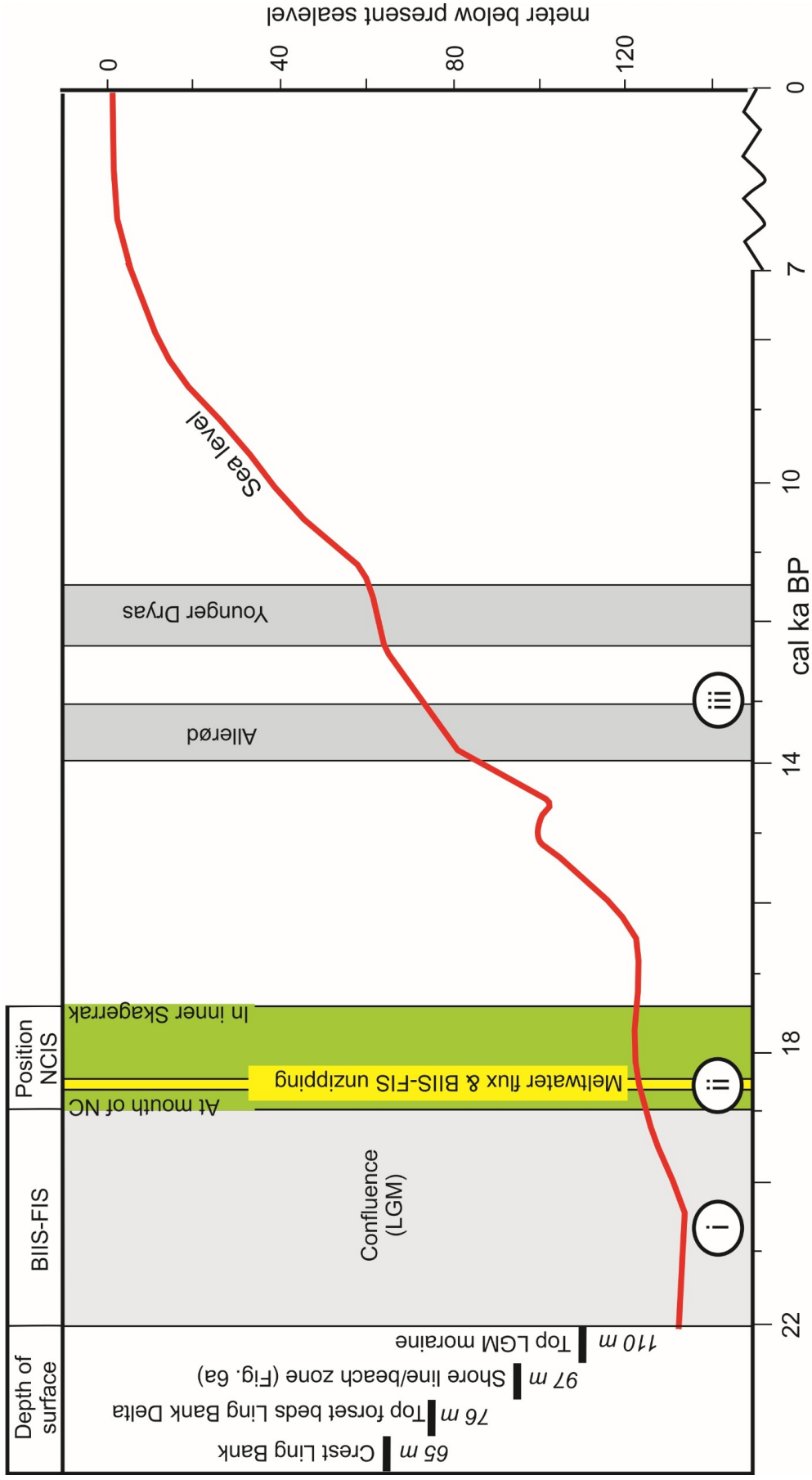


Figure 12. Hjelstuen et al.



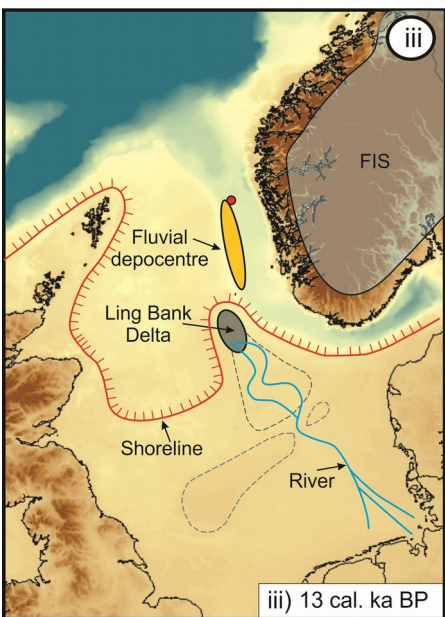
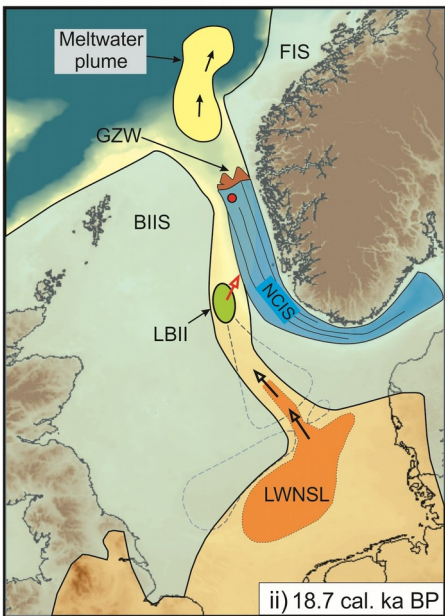
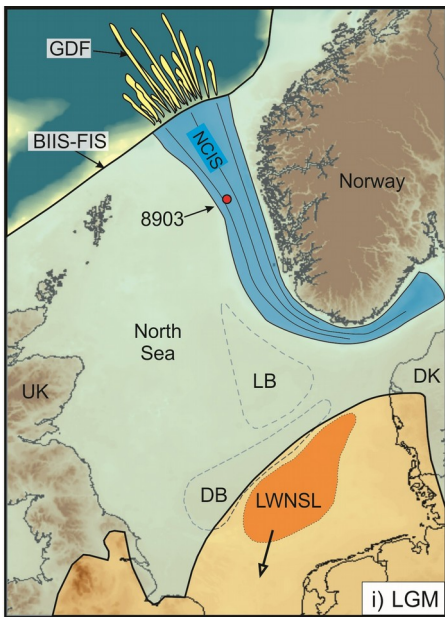


Figure 13. Hjelstuen et al.